

## **Tropospheric Ozone Over the North Pacific From Ozonesonde Observations**

S. J. Oltmans<sup>1</sup>, B. J. Johnson<sup>1</sup>, J. M. Harris<sup>1</sup>, A. M. Thompson<sup>2</sup>, H. Y. Liu<sup>3</sup>, H. Vömel<sup>1,4</sup>,  
C. Y. Chan<sup>5</sup>, T. Fujimoto<sup>6</sup>, V. G. Brackett<sup>7</sup>, W. L. Chang<sup>8</sup>, J.-P. Chen<sup>9</sup>, J. H. Kim<sup>10</sup>, L. Y.  
Chan<sup>5</sup>, H.-W. Chang<sup>11</sup>

<sup>1</sup>NOAA, Climate Monitoring and Diagnostics Laboratory, 325 Broadway, Boulder, CO  
80305, [samuel.j.oltmans@noaa.gov](mailto:samuel.j.oltmans@noaa.gov)

<sup>2</sup>NASA Goddard Space Flight Center, Code 916, Greenbelt, MD 20771

<sup>3</sup>National Institute of Aerospace, Hampton, VA 23666

<sup>4</sup>CIRES, University of Colorado and NOAA/CMDL, Boulder, CO 80309

<sup>5</sup>Dept. of Civil and Structural Engineering, The Hong Kong Polytechnic University,  
Hung Hom, Hong Kong, China

<sup>6</sup>Japan Meteorological Agency, Tokyo, Japan

<sup>7</sup>SAIC, NASA/LaRC, Hampton, VA 23681

<sup>8</sup>Hong Kong Observatory, Hong Kong, China

<sup>9</sup>National Taiwan University, Taipei, Taiwan

<sup>10</sup>Pusan National University, Pusan, Korea

<sup>11</sup>Central Weather Bureau, Taipei, Taiwan

Submitted to the *Journal of Geophysical Research - Atmospheres*

TRACE-P Special Section

January 2003

ABSTRACT: As part of the TRACE-P mission, ozone vertical profile measurements were made at a number of locations in the North Pacific. At most of the sites there is also a multi-year record of ozonesonde observations. From seven locations in the western Pacific (Hong Kong; Taipei; Jeju Island, Korea; and Naha, Kagoshima, Tsukuba, and Sapporo, Japan), a site in the central Pacific (Hilo, HI), and a site on the west coast of the U.S. (Trinidad Head, CA) both a seasonal and event specific picture of tropospheric ozone over the North Pacific emerges. At all of the sites there is a pronounced spring maximum through the troposphere. There are, however, differences in the timing and strength of this feature. Over Japan the northward movement of the jet during the spring and summer influences the timing of the seasonal maximum. The ozone profiles suggest that transport of ozone rich air from the stratosphere plays a strong role in the development of this maximum. During March and April at Hong Kong ozone is enhanced in a layer that extends from the lower free troposphere into the upper troposphere that likely has its origin in biomass burning in northern Southeast Asia and equatorial Africa. During the winter the Pacific subtropical sites (latitude ~25N) are dominated by air with a low-latitude, marine source that gives low ozone amounts particularly in the upper troposphere. In the summer in the boundary layer at all of the sites marine air dominates and ozone amounts are generally quite low (<25 ppb). The exception is near large population centers (Tokyo and Taipei but not Hong Kong) where pollution events can give amounts in excess of 80 ppb. During the TRACE-P intensive campaign period (February-April 2001) tropospheric ozone amounts were rather typical of those seen in the long-term records of the stations with multi-year soundings.

## Introduction

The North Pacific basin is surrounded by major population and industrial centers in Asia and North America. Continental Asia and western coastal North America are known to be major sources of emissions of compounds that are precursors to ozone formation. In addition the North Pacific is a dynamically active region with major storm tracks that often carry cyclonic disturbances from Asia toward North America. These disturbances are a significant mechanism for exchange from the stratosphere into the troposphere. In addition the large anticyclone located over the Pacific sends air from Asia toward North America. The transport patterns have a strong seasonal variation so that transport across the Pacific from Asia toward North America is strongest during the winter and spring months while transport from tropical and subtropical to more northerly latitudes is dominant during the summer.

Ozone is unique among the reactive atmospheric constituents in that it is relatively easily measured and there are at least some regular measurements over longer periods of time. Vertical profiles of ozone were measured using ozonesondes at nine locations over the North Pacific during the Transport and Chemical Evolution over the Pacific (TRACE-P) period. Seven of these sites have multi-year records that have observations throughout the course of the year. Seven of the nine sites were located in the western Pacific consistent with the major focus of TRACE-P [Jacob et al., 2003]. One site was located in Hawaii and another on the western coast of northern California. Information on the location and observation record of the ozonesonde sites is summarized in Table 1. Ozone was measured using electrochemical sensors coupled with meteorological radiosondes flown on balloons. Most observations were done on a weekly

schedule with some enhancements during the period of aircraft observations of TRACE-P. Extensive information on ozonesonde performance can be found in Harris et al. (1998). Under most circumstances the accuracy of ozonesonde measurements is about 10% in the troposphere. To identify dominant transport pathways, isentropic trajectories were calculated for several of the sites. These trajectories were used both for study of individual features seen in the ozone profile and to give a climatological picture of the airflow regimes influencing a particular site. The method for calculating the trajectories as well as a discussion of their limitations are discussed in Harris and Kahl [1994]. An objective clustering technique [Moody, 1986] was used to determine flow patterns for each month at several sites based on a 10-year climatology of ECMWF meteorological fields. With individual cases the NCEP-NCAR reanalysis [Kalnay et al., 1996] was used since data were available at greater height and time resolution (every six hours) for the three hour trajectory calculation time step. Potential vorticity (PV), used to help identify the presence of stratospherically influenced air in the troposphere, was taken from the NCEP reanalysis data.

The approach used here is to look at the stations with multiyear records to define climatological features such as the seasonal variation, provide a context for the TRACE-P aircraft field campaign by comparing the February-April 2001 period with the longer term record for February-April, and finally to look at individual profiles where interesting features may be indicative of particular processes. The longer-term measurements provide a context for the shorter field campaign measurements by helping determine the representativeness of a particular year, and also by placing these observations within the prominent seasonal variation. In comparing measurements from campaigns that may have

taken place in the same general season such as TRACE-P in 2001 and PEM-West B [Davis et al., 1997] in 1994 these longer-term measurements help in judging whether a difference of a couple weeks during a time of rather rapid seasonal change influences the comparisons [Davis et al., 2003].

### Seasonal Variation

Several recent publications have presented global climatologies of tropospheric ozone based primarily on ozonesonde observations [Logan, 1999; Fortuin and Kelder, 1998]. These papers made use of the four Japanese station network of ozone profiles measurements. These observations are also an important part of the picture presented in this work. As with every location where observations have been made, the four Japanese stations, ranging in latitude from 43N to 26N, show a prominent seasonal variation in the troposphere (Figure 1). Through most of the troposphere there is a prominent spring maximum, but beyond this general statement there are numerous differences in detail that are of equal importance. At the highest latitude location (Sapporo) the maximum below 5 km (note the expanded altitude scale for this panel) comes in late April but the peak values are not particularly large (less than about 70 ppbv). Above 5 km the maximum occurs during the summer and the highest values above 8km are associated with the rising altitude of the tropopause (plotted as the thin solid black line). At Tsukuba (36N) the seasonal maximum through most of the troposphere extends from April to June with the largest amounts in June. A notable feature is the very high ozone mixing ratios in the layer below 2km that extends throughout the summer. Such a feature is highly suggestive of local ozone production resulting from precursor emissions in the Tokyo urban plume.

At Kagoshima (32N) there is a strong seasonal maximum in May throughout the troposphere. In June below 5km there is a sharp transition to lower ozone values that are accompanied by a sharp rise in humidity (not shown). This results from the switch to airflow from a more southerly, oceanic sector. This is even more prominent at Naha (26N) where the appearance of maritime air leads to very low summer ozone amounts in the lower troposphere. Naha also shows the characteristic subtropical pattern of low ozone amounts extending into the upper troposphere during late autumn and winter months. This feature is also seen at Hong Kong (22N) and Taipei (25N), which are close in latitude to Naha [Chan et al., 1998; Liu et al., 2002]. At all of these sites there is a gradient with altitude with higher ozone amounts closest to the tropopause and lower amounts near the surface with the notable exception of the low altitude maximum below 2km at Tsukuba. The most prominent extension of high ozone from the upper troposphere deep into the lower troposphere is seen at Kagoshima in May. At altitudes above about 5 km there appears to be a slight lag in the appearance of the seasonal maximum as one goes northward from Kagoshima to Sapporo with the highest values appearing in May at Kagoshima, May-June at Tsukuba, and June-July at Sapporo. This may reflect the northward movement of the subtropical upper tropospheric wind maximum (jet) and the likelihood of stratosphere-troposphere exchange. Further discussion of the source of the spring maximum is dealt with after considering the behavior at other north Pacific sites.

During the winter season (December-January-February) the four Japanese stations have almost identical ozone mixing ratios (Figure 2) at altitudes lower than 7 km. Above 7 km the influence of the height of the tropopause dominates the differences with the

subtropical station at Naha showing a relative minimum at about 13 km. The higher latitude stations of Tsukuba and Sapporo show a sharp rise in mixing ratios above 8 km. In the spring (March-April-May) the ozone amount below about 8 km increases at all stations (Figure 2) but with the highest latitude station (Sapporo) lagging behind. By summer (June-July-August) there is a clear separation between the two higher latitude and two lower latitude Japanese sites. At Naha below 5 km the ozone amounts are less than 30 ppbv with an average mixing ratio under 10 ppbv near the surface. At both Kagoshima and Tsukuba there is a relative maximum at about 1 km that likely reflects the influence of ozone produced in the urban pollution plume. The seasonal maximum between 4-8 km at the two more northerly sites comes during this time of year. By autumn (September-October-November) the ozone amounts below 9 km at these sites is closer together with increasing amounts at the two lower latitude locations and decreasing amounts the higher latitude sites.

At Hong Kong (22N) several of the features of the seasonal pattern (Figure 3) are similar to those seen at Naha. A significant difference is the very pronounced enhancement in ozone seen during late March and April in the 2-10 km layer over Hong Kong. This feature appears to be distinct from the broader seasonal maximum in the upper and middle troposphere. Such a feature may be weakly present at Naha but it does not show a clear separation from the broader seasonal maximum. This enhancement is considered in more detail in the discussion of individual profiles in a later section.

Hilo, Hawaii (20N) has many characteristics of a tropical location with ozone through most of the troposphere at most times of the year being relatively low (<50 ppbv) and values less than 10 ppbv during the summer in the marine boundary layer (Figure 3).

However, in the spring ozone is enhanced to in excess of about 70 ppbv above 5 km. Between 13-16 km from March through June the influence of the stratosphere appears to predominate with average amounts greater than 90 ppbv. Some of the features seen at the west coast U.S. location (Figure 3) at Trinidad Head, California (41N) resemble those seen on the opposite side of the Pacific at Sapporo, but there are also some differences. At both locations the seasonal maximum in the mid-troposphere is broad. At both sites there are large ozone amounts in the upper troposphere and large tropospheric amounts are seen to highest altitudes during the summer as the tropopause height pushes upward. In the spring through the summer there is about a 2 km thick layer just below the tropopause with ozone in excess of about 125 ppbv.

#### Comparison between the western and eastern north Pacific

Located between the latitudes of Tsukuba and Sapporo, Trinidad Head more nearly resembles the ozone amounts and seasonal pattern seen at Tsukuba (Figure 4). In the winter below 6 km the ozone amounts at Trinidad Head and Tsukuba are similar (there is less ozone at Sapporo), but above the lower tropopause heights over Japan seem to be responsible for more ozone at these altitudes. In the spring Tsukuba and Trinidad Head are quite similar with slightly more ozone at Tsukuba below 3 km and above 6 km. These differences may not be significant, however, given the level of variability and the fact that the periods of record are not the same with only about 5 years of observations at Trinidad Head compared with the 10-year record used for this study for the Japanese stations. At Sapporo the spring ozone amount below 6 km is identical to that at Trinidad Head. Summer is the season of the largest differences with the strong enhancement in the

lower troposphere at Tsukuba not seen at Trinidad Head. In the lower troposphere during the summer the amounts at Trinidad Head match those at Sapporo, which is another indication of the local influence on the enhancement seen at Tsukuba. At Tsukuba, and even more so at Sapporo, there is more ozone above 3 km in the western than in the eastern Pacific. In the autumn the ozone amount throughout the depth of the troposphere is nearly the same at Tsukuba and Trinidad Head. Based on the average seasonal behavior described here there is no evidence for significant west to east gradients in tropospheric ozone below 6 km at mid-latitudes over the North Pacific. Above this altitude there is more ozone only in the winter in the western Pacific and this appears to be primarily associated with the height of the tropopause. In general the gradients seen across the Pacific are smaller than those seen across the continental U.S. (Newchurch et al., 2003).

#### Transport patterns to the ozonesonde sites

Seasonal ozone characteristics were investigated in relationship to average flow patterns to several of the sites. The transport to Kagoshima, Hilo, and Trinidad Head was characterized using a 10-year trajectory climatology to determine if the seasonal variation was associated with differences in air transported to a particular site. The individual trajectories are clustered to give representative transport paths (Moody et al., 1986). The three sites were chosen to illustrate these patterns in the western, central and eastern Pacific. At Kagoshima the spring season shows a rapid buildup of ozone throughout the troposphere peaking in May. In the autumn on the other hand the September-November ozone amounts are quite similar and in fact remain rather similar through February

(Figure 1). The flow patterns at various altitudes for the individual seasons do not give a consistently clear indication of a shift in flow regimes that accounts for the strong difference in ozone amounts during the spring and the autumn-winter seasons. This suggests that other processes such as chemical formation play a significant role. At the lower altitudes (1 km) and higher altitudes (12 km) there is more of tendency for the seasonal ozone change to be related to the transport path. The spring and summer seasons show the strongest contrast in ozone (Figure 5) and also a large difference in transport pattern (Figure 6). At 4 km during May (Figure 6a) there is no trajectory cluster in which air parcels remain over the ocean for a significant fraction of their travel time while in August (Figure 6b) 55% remain over the ocean for the full 10 days of the computed trajectory. The average ozone mixing ratio in May is 40 ppbv higher than in August at 4 km and reflects the significant ozone sink in the low latitude, summer marine atmosphere. At other altitudes, trajectories that remain over the ocean for the full 10 days are seen at least 45% of the time (at 12 km) to a high of more than 75% (at 1 km) in August. In May, on the other hand, only in the boundary layer do trajectories remain over the ocean (20% of the time).

At Hilo, where through almost all of the troposphere there is a sharp April peak and broad seasonal minimum that stretches from July through September (Figure 3), several important transport differences are apparent. On average over the year and at all altitudes a large fraction of the trajectories spend 10 days over the Pacific Ocean prior to reaching Hawaii, ranging from more than 75% at 1 km to greater than 45% at 4 km. In the two months with the strongest contrast in ozone amount (Figure 7) at all altitudes (April and September) there are also differences in the transport pattern (Figures 8a and

8b). In September (Figure 8b) at all altitudes at least 90% of the trajectories remain over the ocean for 10 days and below 4 km (Figure 8) essentially all spend 10 days over the ocean. In April over-ocean trajectories are still prominent at low altitudes but, for example, at 4 km (Figure 8a) almost half reach the Asian continent, primarily China near 30°N. At 8 and 12 km more than 80% of the trajectories in April go back over southern China and Southeast Asia at latitudes lower than 30°N. During April this is a significant biomass burning region with large enhancements of ozone [Liu et al., 1999, Chan et al., 2000] which may contribute to the seasonal ozone enhancement seen in Hawaii [Liu et al., 2002]. During the winter months there is also significant flow from Asia to Hawaii but this does not significantly enhance ozone amounts, due to the reduced photochemical activity during this season.

The eastern Pacific site at Trinidad Head, is at a somewhat higher latitude (41N) than the central and western Pacific sites and this is reflected in the flow pattern which is dominated by westerly winds for much of the year. As noted earlier there is a broad spring-early summer maximum in ozone through most of the troposphere (Figure 3) while winter months are very consistent with mixing ratios of about 40-50 ppbv from above the marine boundary layer through the upper troposphere. The contrast between the seasons in ozone amount is not as sharp as at Kagoshima and Hilo, and this is reflected in the trajectories where the differences in transport pattern are not as great between the seasons (Figure 9). Both in May and November at 4 km 40-50% of the trajectories to Trinidad Head remain over water for 10 days and at 8 km about 30% do not reach a landmass in 10 days. At low altitudes in the marine boundary the primary contrast in transport is between the spring and summer with about 25% more trajectories

reaching land in spring. At low altitudes the trajectories that do go back over land come mostly from north of  $45^{\circ}\text{N}$ . In both May (Figure 10a) and November (Figure 10b) there is a significant cluster of trajectories that pass over central Japan and over the Yellow Sea at 4 km with November having about twice as many such trajectories as May. In both months there is also  $\sim 8\%$  of the trajectories that come from latitudes higher than  $60^{\circ}\text{N}$  and show significant subsidence. In May such trajectories are likely to bring upper tropospheric air that has enhanced ozone from the stratosphere while in November the upper troposphere is not so enhanced in ozone because of weaker exchange from the stratosphere [Danielsen and Mohnen, 1977]. The major factor controlling the seasonal difference in ozone amount in much of the troposphere at Trinidad Head appears not to be the differing transport regimes but rather the fact that in the spring and early summer both the photochemistry and transport from the stratosphere are enhanced over what is present in the winter months. In the boundary layer during the summer the fact that air stays almost exclusively over a relatively clean ocean region appears to lead to ozone loss, so that below about 1 km ozone amounts are about 5 ppbv (20%) lower in the summer than in the winter and spring.

#### Representativeness of the TRACE-P aircraft campaign period

The two TRACE-P aircraft operated in the western Pacific from late February through early April 2001. In the first half of the period the planes operated out of Hong Kong and in the latter half from near Tokyo, Japan. Shown here are the February-April 2001 averages compared with the longer-term 10-year record from one of the Japanese sites and the approximately 5-year record from Hong Kong (Figure 11). Of course the

aircraft did not operate near any of these locations for the entire period so that the purpose here is to discern major differences between the tropospheric regime sampled in 2001 compared to the “average” behavior. The differences are minor with the only significant difference in the upper troposphere at Hong Kong (Figure 11) where there was a pronounced minimum at about 13 km in 2001 that is not seen in the longer-term average. This minimum was also present at Taipei during 2001 (not shown), although not as pronounced as at Hong Kong, indicating that this was not just a sampling artifact at a single site. Trajectories for the individual profiles at the altitude of this upper tropospheric minimum show strong transport from the equatorial western Pacific for a number of the cases. The corresponding outgoing longwave radiation (OLR) shows reduced OLR corresponding to significant convection over the region that the trajectories traverse (<http://www.cdc.noaa.gov/HistData/>). It is likely that the air seen in the upper troposphere over Hong Kong and Taipei in many of the profiles in February – April 2001 has a source in the equatorial boundary layer. The prevalence of such profiles in 2001 appears to be responsible for the minimum seen at 13 km in the average and reflects the lingering influence of the cold phase of ENSO [Liu et al., 2003].

#### Individual cases

Several individual case studies were examined for flow characteristics or unique features that might identify the origin of the feature. As noted earlier during the month of May Kagoshima has a very pronounced maximum in ozone through the entire troposphere in comparison with other months. The individual profiles are often marked by layers of enhanced ozone that exceed 100 ppbv. Three individual profiles (Figure 12)

were chosen that are representative of many of the May profiles over the 10-year climatology used in this study. In all three cases the local tropopause (thermal) was at an altitude greater than 15 km, which is the usual case for May (see Figure 3). On May 20, 1999 there is an overall increase in ozone mixing ratio from ~40 ppbv at the surface to ~130 ppbv at 16 km. This "background" profile is similar to the long-term average for May (Figure 5). Superimposed on the "background" profile are prominent peaks at approximately 3, 7, 10, and 12 km with peak mixing ratios of 88, 133, 126, and 139 ppbv, respectively. At 3 km air has traveled rapidly from the north and descended significantly prior to reaching Kagoshima (Figure 13). Air parcel trajectories at 0000 and 0600 GMT show even more dramatic descent of 4 km in the two days prior to reaching the site. This corresponds with a strong surge of cool, dry air from Siberia. This layer has the marks of air that has recently descended from the stratosphere [Cooper et al., 1998]. The layer at 7 km also is very dry and has also descended (3 km) from aloft. On May 17, 2000 at the ozone peak layer at 7 km the trajectory is very similar to the May 20, 1999 trajectory for a layer at the same altitude with descent of 3 km in the final two days before reaching Kagoshima (Figure 14). Each of these trajectories indicates that the air parcel has passed through a region of high potential vorticity (PV) within 1-3 days prior to arriving at the site. The PV in the layer of high ozone mixing ratio is also enhanced. On May 29, 2000 the air parcels in the layer at 4 km have also descended rapidly more than 5 km in the two days prior to reaching Kagoshima. There are not elevated PV values in this layer at the time of the sounding. The air parcel travels from high latitudes and encounters a region of higher PV about a week before arriving at Kagoshima. The complex path of the trajectory earlier than the three days prior to reaching the site makes the identification of a source

difficult. The air parcel also descends over the Yellow Sea through a region of significant ozone precursor sources that may contribute to the ozone loading in this layer. In this case a mixture of sources may be responsible for the elevated ozone amounts seen in this layer. In the layer from 6-10 km of relatively low ozone amounts on May 29 the trajectories stay at latitudes south of Kagoshima passing over China, northern India and Africa, and the Atlantic. The trajectories or other meteorological data do not suggest a particular source of the lower ozone air other than the air parcels generally remaining at subtropical latitudes.

At Hong Kong the February-April time frame is a period when the tropospheric ozone distribution is altered by biomass burning (Liu et al., 1999). The layer at 3 km in the profile of March 17, 2000 (Figure 15) shows a transport pattern representative of profiles with an enhancement near this altitude. The air parcel trajectory (Figure 16) comes over northern Southeast Asia with a travel time of about two days after remaining relatively stagnant during the previous several days. This pattern is typical (Liu et al., 1999, 2002) of the layer of high ozone amounts seen over Hong Kong that results from biomass burning over northern Southeast Asia. Plumes of enhanced ozone are not confined to the lower free troposphere but may also appear at substantially higher altitudes as is seen on March 16, 2001 (Figure 15). The trajectory (Figure 17) also shows the air parcel traveling over northern Indochina, extending over India, and within ~5 days to northern Africa. Significant lifting of the air parcel is also necessary to form a layer at this altitude if the source of the ozone and/or its precursors is within the boundary layer. The source of the enhanced ozone amounts in the layer at 9-10 km over Hong Kong is not clear from the trajectory alone. Examination of the outgoing longwave radiation

(OLR) information shows little evidence of convection over northern Southeast Asia in the 1-2 days prior to the observation of the enhanced ozone layer over Hong Kong.

Northern equatorial Africa is also a region of significant biomass burning during this time of year and can also have significant convection. An ozone profile was obtained at Taipei on March 16, 2001 as well (Figure 18). An enhanced ozone layer was also seen at 9 km in this profile and the trajectory (Figure 19) looks very similar to that at Hong Kong with very rapid transport from northern Africa.

A profile on March 27, 2001 launched at 0515 GMT (Figure 15) over Hong Kong has both the lower and higher altitude features in a single profile and provides an opportunity to look at the possible contributing causes to the ozone enhancements. The trajectories at 3 km and 10 km (Figure 20) are very similar to those seen for the two other profiles for the corresponding layers. At 3 km (Figure 20a) the trajectory path stagnates over northwestern Myanmar and then moves rapidly over northern Vietnam while ascending to the 3 km altitude where the enhanced ozone peak is seen over Hong Kong. The fire count map for March 2001 (<http://shark1.esrin.esa.it/ionia/FIRE/AF/ATSR/>) shows that the most intensive burning in Southeast Asia during this month was in western Myanmar (Figure 21), which is the origin of the air parcel reaching Hong Kong based on the trajectory calculation. For the 9-11 km layer at Hong Kong on March 27, 2001 the air parcel trajectory for 0600 GMT passes over Southeast Asia, India and the Arabian Peninsula within two days reaching central Africa within three days (Figure 20b). West-central equatorial Africa is both a region of burning (Figure 17) [Duncan et al., 2003] and of convection based on the low values of OLR (Figure 22). Tropospheric column ozone is also enhanced near the region of high fire counts and convection in Nigeria based on

the Tropical Tropospheric Ozone (TTO) map (Figure 23) from the TOMS observations [Thompson and Hudson, 1999]. Very high TTO is also seen near the horn of Africa, which is the region that trajectories for the soundings of March 16, 2001 at Hong Kong and Taipei show as a possible source of the enhanced layer. Although the TTO maps for the time corresponding to these soundings do not show such impressive enhancements, it appears from the fire counts and the TTO maps that this region can be a significant source region for ozone. On the other hand there is little evidence of convection based on OLR over northern Southeast Asia, or India in the 1-2 days prior to the air parcel reaching Hong Kong. Because it was not possible to match fires with convection along the trajectory path in a precise way the influence of African burning on the ozone profile over Hong Kong is suggestive but not conclusive. There is, however, a good deal of consistency in the airflow patterns and source regions that produce the enhanced ozone layers over Hong Kong. The influence of biomass burning in Africa as well as lightning were found to contribute to enhanced ozone in the upper troposphere at Hong Kong by Liu et al. [2002]. A modeling study [Liu et al., 2003] that looks at CO transport for observations made as part of the DC-8 aircraft measurements in TRACE-P on March 26, 2001 to the east of Hong Kong suggests that an enhanced layer of upper tropospheric CO was a result of convection over Southeast Asia. The OLR for March 25 shows strong convection over southern Laos. This is consistent with finding of Liu et al. [2002] that S.E. Asian burning is an important source of upper tropospheric ozone enhancements over Hong Kong. It appears that transport in the upper troposphere at Hong Kong can alternate between two regimes – a low latitude regime with transport from S. E. Asian burning or westerly flow influenced by equatorial African sources.

A striking feature of the Taipei profile of March 16, 2001 (Figure 18) is the layer of very high ozone amount below 2 km. A similar feature is not seen at Hong Kong. Trajectories at the altitude of the maximum at Taipei (Figure 24) are similar for both Hong Kong and Taipei. Both show air moving southward from China to the west of Korea over the Yellow Sea, a region noted for high levels of pollution. This trajectory shows very rapid descent of ~ 5 km as the air parcel leaves the coast. The trajectory passes through a slightly enhanced region of PV just north of the Yellow Sea as the air parcel begins its sharp descent. A CTM modeling study (Wild et al., 2003) shows that in addition to the significant pollution produced ozone there is a strong stratospheric ozone signal associated with air descending on the back side of the cold front that passes over Taipei.

During the summer at Taipei (Figure 18) very high ozone amounts (>100 ppbv) are common in the lowest 2 km. Unlike the case in March 2001, however, there is not an indication of flow from mainland China but rather very weak circulation coming from off the ocean. This suggests that these are local urban pollution events resulting from the emission of precursors in the immediate region. A very similar pattern is seen at Tsukuba, Japan as was noted earlier. Such local pollution events are seen at Hong Kong during the summer but less frequently than at Taipei.

At Jeju Island in the Yellow Sea off the southwest coast of Korea the profile of March 1, 2001 (Figure 25) has prominent maxima at 5.5 km and 9 km with elevated ozone amounts from 4 km up to the tropopause. This enhancement is associated with stratosphere-troposphere exchange that is well simulated by a CTM (Wild et al., 2003). The stratospheric origin of the air can be seen clearly in the PV map (Figure 26a) for

0600 GMT at a potential temperature ( $\Theta$ ) of 300 K (the potential temperature surface where the 5.5 km layer is seen at Jeju) where a tongue of high PV stretches down over Korea. At  $\Theta = 330$  K (where the 9 km layer is seen) very high PV is seen well south of Korea and over Japan (Figure 26b). There is no sounding at Kagoshima at this time but there is one at Tsukuba on March 2, 2001 with very high ozone (>300 pbbv) just above 7 km which is at  $\Theta = 300$  K. By March 2 the large ozone amounts are confined to altitudes above 10 km (the  $\Theta = 330$  K surface is in the stratosphere at  $\sim 11$  km) at Jeju as the system responsible for the exchange event has moved rapidly eastward but ozone amounts are still very high over Japan.

At Hilo ozone profiles were obtained on both March 15 and 16, 2001 (Figure 27) showing a prominent peak of 100 pbbv in ozone mixing ratio centered at 8 km on March 15 diminishing somewhat to  $\sim 85$  pbbv on March 16. March 16 was the day that enhanced ozone amounts were seen at 9 km in the profile at Hong Kong and Taipei. The measurements at Hilo ( $\sim 1830$  GMT each day) bracket the time of the soundings at Hong Kong and Taipei ( $\sim 0600$  GMT on March 16). The trajectory for the air parcel reaching Hilo at 1800 GMT on March 15 and March 16 show the air parcel reaching the coast of China in about four days, well before the time of the soundings in Hong Kong and Taipei. A profile at 0245 GMT at Taipei on March 13 and another on the same day at Hong Kong at 0530 GMT each showed only a modest enhancement ( $\sim 75$  pbbv) at about 9 km. Since the trajectory to Hilo went north of both Hong Kong and Taipei by  $\sim 5^\circ$  in latitude and 2-3 days earlier, the ozone peak at Hilo was probably not related to the same series of events leading to the ozone peaks seen at Hong Kong and Taipei. The PV map for March 15 shows a band of enhanced PV stretching from the coast of California westward to

encompass Hawaii (Figure 28) near the altitude of the layer of high ozone observed in the soundings of March 15 and 16. This feature becomes a cutoff region of enhanced PV on March 16 over southern Hawaii.

In the spring at Trinidad Head there is strong westerly flow in the upper troposphere that brings air directly from over Asia (Figure 10a). In general the ozone profiles associated with such transport do not show remarkable excursions. Prominent peaks are seen in profiles such as the one for March 9, 2001 (Figure 28) and are often associated with descending air parcels from the northwest (Figure 30). Potential vorticity (PV) in the 6-9 km layer (Figure 31) is greatly enhanced over tropospheric values. In addition the PV three days prior to the sounding at Trinidad Head is very high at the time the trajectory shows the air parcel passing over Japan in the layer where high ozone mixing ratios are measured at Trinidad Head. These trajectories pass over Japan and China but there is little indication of a mechanism for lofting air to the altitude where ozone enhancement is seen. A low pressure system to the east of Japan and associated stratosphere-troposphere exchange on the flank of this low is the likely source of the ozone layer at 6-9 km seen at Trinidad Head.

## Conclusions

Ozone profiles over the north Pacific generally show a prominent spring maximum throughout the troposphere. This maximum is tied to the location of the jet and its influence on stratosphere-troposphere exchange, and the increase in photochemical ozone production through the spring. Prominent layers of enhanced ozone in the middle and upper troposphere north of about 25°N seem to be more closely tied to stratospheric

intrusions while biomass burning leads to layers of enhanced ozone in the lower and upper troposphere at Hong Kong and Taipei. The lower free tropospheric layers at Hong Kong are associated with burning in S.E. Asia while the upper layer may be associated with either equatorial N.H. burning in Africa or S. E. Asian biomass burning. In the boundary layer at Taipei very high mixing ratios of ozone were observed that result from pollution transport from China in the spring and local urban pollution during the summer. At the ozonesonde site near Tokyo very large enhancements of ozone are seen in the boundary layer in the summer that are characteristic of urban air pollution. At sites in the mid and eastern Pacific the signature of transport of polluted air from Asia is not readily identifiable from the ozonesonde profile. This is likely due to the more subtle signal and the fact that from the ozone profile and meteorological data by themselves it is difficult to identify such a signal. Additional tracer data not available from the ozonesonde measurements is required.

## References:

- Chan, L. Y., H. Y. Liu, K. S. Lam, T. Wang, S. J. Oltmans, and J. M. Harris, Analysis of the seasonal behavior of tropospheric ozone at Hong Kong, *Atmos. Environ.*, 32, 159-168, 1998.
- Chan, L. Y., C. Y. Chan, H. Y. Liu, S. Christopher, S. J. Oltmans, and J. M. Harris, A case study on the biomass burning in Southeast Asia and enhancement of tropospheric ozone over Hong Kong, *Geophys. Res. Lett.*, 27, 1479-1482, 2000.
- Cooper, O. R., J. L. Moody, J. C. Davenport, S. J. Oltmans, B. J. Johnson, X. Chen, P. B. Shepson, and J. T. Merrill, Influence of springtime weather systems on vertical ozone distributions over three North American sites, *J. Geophys. Res.*, 103, 22,001-22,013, 1998.
- Danielsen, E. F. and V. A. Mohnen, Project Dustorm report: Ozone transport, in situ measurements and meteorological analyses of tropopause folding, *J. Geophys. Res.*, 82, 5867-5877, 1977.
- Davis, D. D. et al., Trends in western North-Pacific ozone photochemistry as defined by observations from NASA's PEM-West B (1994) and TRACE-P (2001) field studies, *J. Geophys. Res. (submitted to TRACE-P Special Section)*, 2003.
- Duncan, B. N., R. V. Martin, A. C. Staudt, R. Yevich, and J. A. Logan, Interannual and seasonal biomass burning emissions constrained by satellite observations, *J. Geophys. Res.*, 4040, doi:10.1029/2002JD0022378, 2003.
- Fortuin, J. P. and H. Kelder, An ozone climatology based on ozonesonde and satellite measurements, *J. Geophys. Res.*, 103, 31,709-31,734, 1998.
- Harris, J. M. and J. D. Kahl, Analysis of 10-day isentropic flow patterns for Barrow, Alaska: 1985-1992, *J. Geophys. Res.*, 99, 25,845-25,855, 1994.
- Hoell, J. M., D. D. Davis, S. C. Liu, R. E. Newell, H. Akimoto, R. J. McNeal, and R. J. Bendura, Pacific Exploratory Mission – West Phase B: February-March, 1994, *J. Geophys. Res.*, 102, 28,223-28,240, 1997.
- Harris, N., R. Hudson and C. Phillips, SPARC/GAW/IOC Assessment of Trends in Vertical Distribution of Ozone, *SPARC Report No. 1 and WMO Ozone Research and Monitoring Project Report No. 43*, Cedex, France, 1998.
- Jacob, D. J., J. H. Crawford, M. M. Kleb, V. E. Connors, R. J. Bendura, J. W. Raper, G. W. Sachse, J. C. Gille, and L. Emmons, The Transport and Chemical Evolution over the Pacific (TRACE-P) aircraft mission: Design, execution, and overview of first results, *J. Geophys. Res.*, (submitted to TRACE-P Special Section), 2003.

Kalnay, E. et al., The NCEP-NCAR 40 year reanalysis project, *Bull. Am. Meteorol. Soc.*, 77, 437-471, 1996.

Liu, H, W. L. Chang, S. J. Oltmans, L. Y. Chan, J. M. Harris, On springtime high ozone events in the lower troposphere from Southeast Asian biomass burning, *Atmos. Environ.*, 33, 2403-2410., 1999.

Liu, H., D. J. Jacob, L. Y. Chan, S. J. Oltmans, I. Bey, R. M. Yantosca, J. M. Harris, B. Y. Duncan, and R. V. Martin, Sources of tropospheric ozone along the Asian Pacific Rim: An analysis of ozonesonde observations, *J. Geophys. Res.*, 107(D21), 4573, doi:10.1029/JD002005, 2002.

Liu, H., D. J. Jacob, I. Bey, R. M. Yantosca, B. N. Duncan, and G. W. Sachse, Transport pathways for Asian combustion outflow over the Pacific: Interannual and seasonal variations, *J. Geophys. Res.*, (submitted to *TRACE-P Special Section*), 2003.

Logan, J. A., An analysis of ozonesonde data for the troposphere: Recommendations for testing 3-D models and development of a gridded climatology for tropospheric ozone, *J. Geophys. Res.*, 104, 16,115-16,149, 1999.

Moody, J., The influence of meteorology on precipitation chemistry at selected sites in the eastern United States, Ph.D. thesis, 176 pp., Univ. of Michigan, Ann Arbor, Michigan, 1986.

Newchurch, M. J., M. A. Ayoub, S. J. Oltmans, B. J. Johnson, F. J. Schmidlin, Vertical distribution of ozone at four sites in the United States, *J. Geophys. Res.* (in press), 2003.

Thompson, A. M. and R. D. Hudson, Tropical Troposphere Ozone (TTO) maps from Nimbus-7 and Earth Probe TOMS by the modified residual method: Evaluation with sondes, ENSO signals and trends from Atlantic regional time series, *Geophys. Res.*, 104, 26,961-26,975, 1999.

Wild, O., J. K. Sundet, M. J. Prather, I. S. A. Isaksen, H. Akimoto, E. V. Browell, and S. J. Oltmans, CTM ozone simulations for Spring 2001 over the Western Pacific: Comparisons with TRACE-P lidar, ozonesondes and TOMS columns, *J. Geophys. Res.* (submitted to *TRACE-P Special Section*), 2003.

Table 1: Locations and period of measurement for ozonesondes in the North Pacific.

<b>Station</b>	<b>Latitude</b>	<b>Longitude</b>	<b>Observations</b>
Hilo, Hawaii	19.4°N	155.4°W	1991-2001
Hong Kong, China	22.2°N	114.3°E	1993-2001
Taipei, Taiwan	25.0°N	121.4°E	2000-2001
Naha, Japan	26.2°N	127.7°E	1991-2001
Kagoshima, Japan	31.6°N	130.6°E	1991-2001
Jeju Island, Korea	33.5°N	126.5°E	2001
Tsukuba, Japan	36.1°N	140.1°E	1991-2001
Trinidad Head, Calif.	40.8°N	124.2°W	1997-2001
Sapporo, Japan	43.1°N	141.3°E	1991-2001

## Figures

Figure 1: Average seasonal variation with altitude of the ozone mixing ratio at four Japanese ozonesonde sites from data for the period 1991-2001. Note the different altitude scale for Sapporo (0-15 km instead of 0-18 km). The solid dark line is the average tropopause height.

Figure 2: Average ozone vertical profiles by season at four Japanese ozonesonde stations. The symbol is the median value at 0.25 km altitude increments. For Kagoshima (x) the inner 50<sup>th</sup> percentile (25<sup>th</sup> to 75<sup>th</sup> percentile) of the data are plotted at each altitude as a horizontal line.

Figure 3: Average seasonal variation of the ozone mixing ratio at Hong Kong, Hilo and Trinidad Head. Note the different altitude scale for Trinidad Head.

Figure 4: Comparison of the seasonal ozone profiles at Tsukuba, Japan and Trinidad Head, California. The symbol is the median value at 0.25 km altitude increments. The inner 50<sup>th</sup> percentile (25<sup>th</sup> to 75<sup>th</sup> percentile) of the data are plotted at each altitude as a horizontal line.

Figure 5: Median monthly tropospheric ozone mixing ratio for May (open triangle) and August (solid diamond) for Kagoshima, Japan. The solid and dotted horizontal lines are the inner 50<sup>th</sup> percentile of the mixing ratio at each 0.25 km altitude.

Figure 6: Average air parcel trajectories at 4 km altitude at Kagoshima for a) May and b) August based on data for 1991 – 2001 determined by clustering twice-daily trajectories. The percentage of the trajectories in each cluster is shown with the corresponding color symbol.

Figure 7: Same as Figure 5 for Hilo, Hawaii for April and September.

Figure 8: Same as Figure 6 for Hilo for a) April and b) September.

Figure 9: Same as Figure 5 for Trinidad Head, California for May and November.

Figure 10: Same as Figure 6 for Trinidad Head for a) May and b) November.

Figure 11: Comparison of the February-March-April 2001 median ozone mixing ratio profiles with the long-term average for Hong Kong and Kagoshima. The inner 50<sup>th</sup> percentile (25<sup>th</sup> to 75<sup>th</sup> percentile) of the data is plotted at each altitude as a horizontal line.

Figure 12: Profiles of ozone mixing ratio at Kagoshima on May 20, 1999, May 17, 2000, and May 29, 2000. The launch time of the ozonesonde for the three profiles was 1430 GMT.

Figure 13: Isentropic 10-day back trajectory to Kagoshima on May 20, 1999 arriving at 3.3 km. The solid line is for the 1200 GMT trajectory and the dashed line for 1800 GMT.

Figure 14: Isentropic 10-day back trajectory to Kagoshima on May 17, 2000 arriving at 7.3 km at 1800 GMT.

Figure 15: Profiles of ozone mixing ratio at Hong Kong on March 17, 2000, March 16, 2001, and March 27, 2001. The launch time of the ozonesonde for the three profiles was ~0530 GMT.

Figure 16: Isentropic 10-day back trajectory to Hong Kong on March 17, 2000 arriving at 3 km. The solid line is for the 0000 GMT trajectory and the dashed line for 0600 GMT.

Figure 17: Same as Figure 16 for March 16, 2001 at 9 km.

Figure 18: Profiles of ozone mixing ratio at Taipei on August 7, 2000 at 0400 GMT and March 16, 2001 at 0700 GMT.

Figure 19: Isentropic 10-day back trajectory to Taipei on March 16, 2001 arriving at 9 km. The solid line is for the 0000 GMT trajectory and the dashed line for 0600 GMT.

Figure 20: Isentropic 10-day back trajectory to Hong Kong on March 27, 2001 at 0060 GMT arriving at a) 3 km and b) 10 km.

Figure 21: Fire counts for March 2001 from the European Space Agency World Fire Atlas compiled from observations made by the Along Track Scanning Radiometer (ATSR) on the ERS-2 satellite. The fire locations are the red dots.

Figure 22: Outgoing Longwave Radiation (OLR) data averaged for the 5-day period March 17-21, 2001 provided by the NOAA Climate Diagnostics Center. Low values of OLR are indicative of thick cloudiness associated with convective activity.

Figure 23: Tropical Tropospheric Ozone (TTO) derived from the Earth Probe TOMS instrument.

Figure 24: Isentropic 10-day back trajectory to Taipei on March 16, 2001 at 0060 GMT at 1 km.

Figure 25: Profiles of ozone mixing ratio at Jeju Island on March 1, 2001 at 0415 GMT and March 2, 2001 at 0615 GMT. The median profile for the eight soundings obtained during March and April 2001 is also shown. The inner 50<sup>th</sup> percentile (25<sup>th</sup> to 75<sup>th</sup> percentile) of the data is plotted at each altitude as a horizontal line.

Figure 26: Potential vorticity on March 1, 2001 at 0600 GMT on the a) 300 K and b) 330 K potential temperature surfaces.

Figure 27: Profiles of ozone mixing ratio at Hilo on March 15 and 16, 2001 at 1830 GMT.

Figure 28: Potential vorticity on March 15, 2001 at 1800 GMT on the 330 K potential temperature surface.

Figure 29: Profile of ozone mixing ratio at Trinidad Head on March 9, 2001 at 1800 GMT. The multiyear median profile for March is also shown. The inner 50<sup>th</sup> percentile (25<sup>th</sup> to 75<sup>th</sup> percentile) of the data is plotted at each altitude as a horizontal line.

Figure 30: Isentropic 10-day back trajectory to Trinidad Head on March 9, 2001 at 1800 GMT arriving at 6 km.

Figure 31: Potential vorticity on March 9, 2001 at 1800 GMT on the 315 K potential temperature surface.

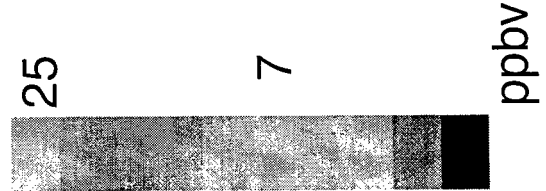
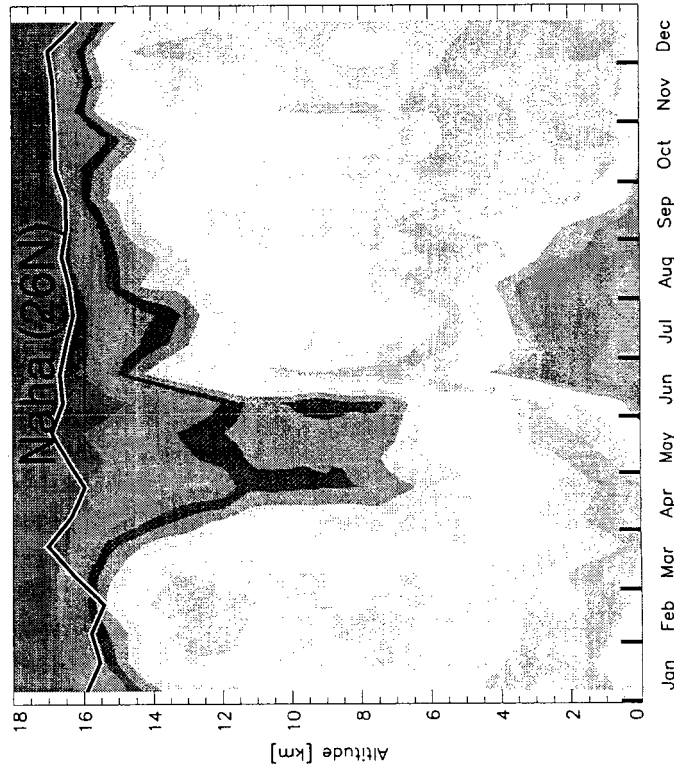
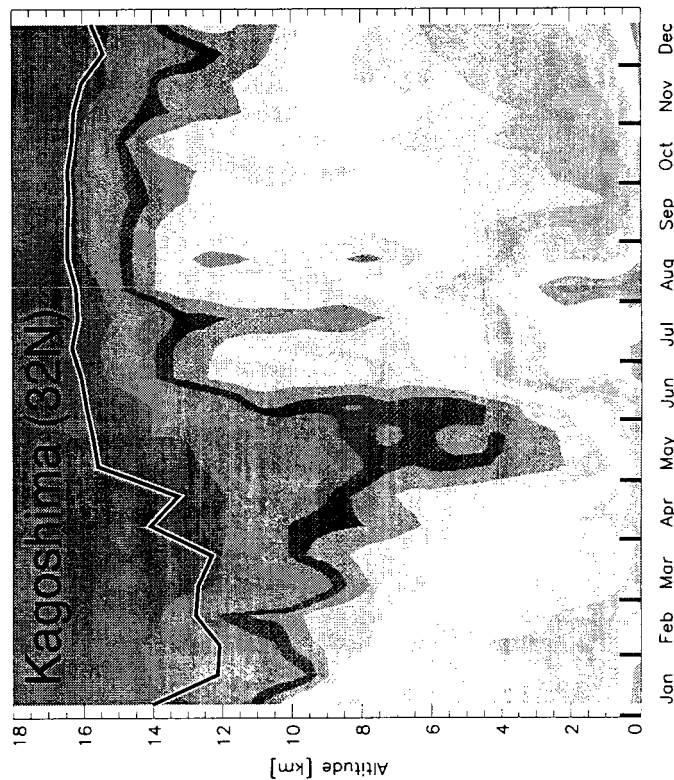
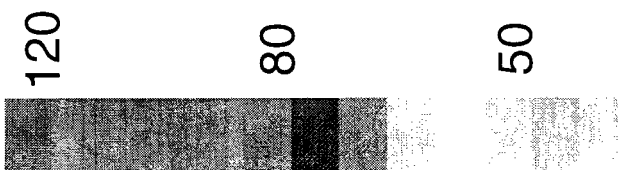
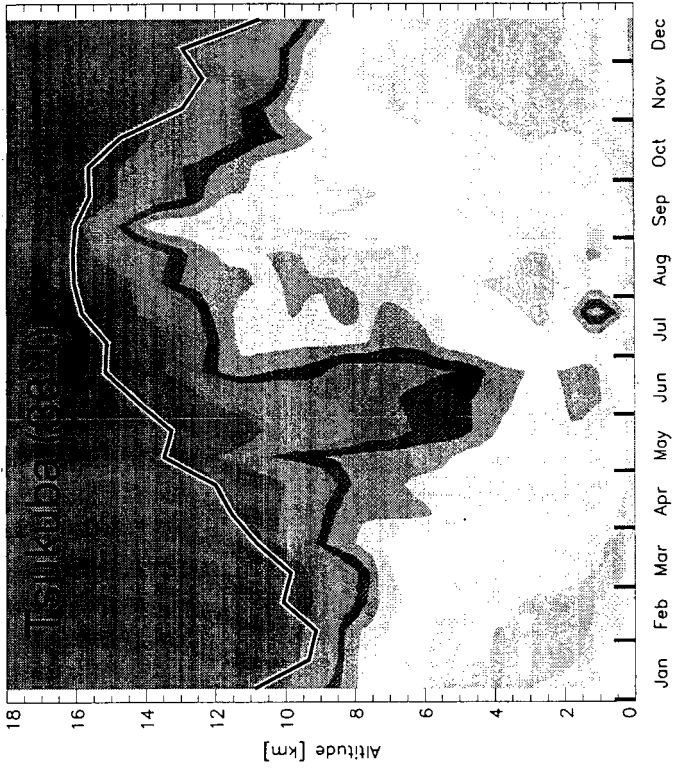
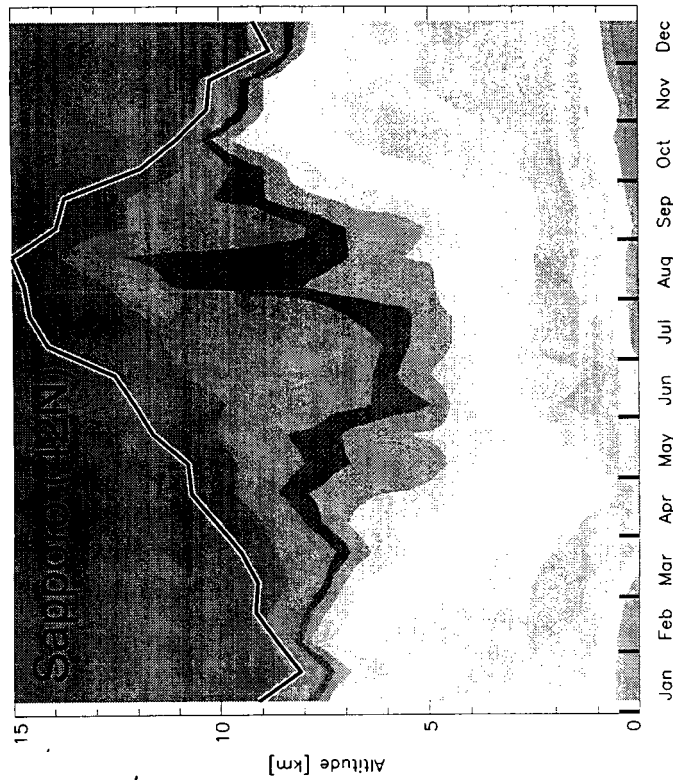


Figure 1: Average seasonal variation with altitude of the ozone mixing ratio at four Japanese ozonesonde sites from data for the period 1991-2001. Note the different altitude scale for Sapporo

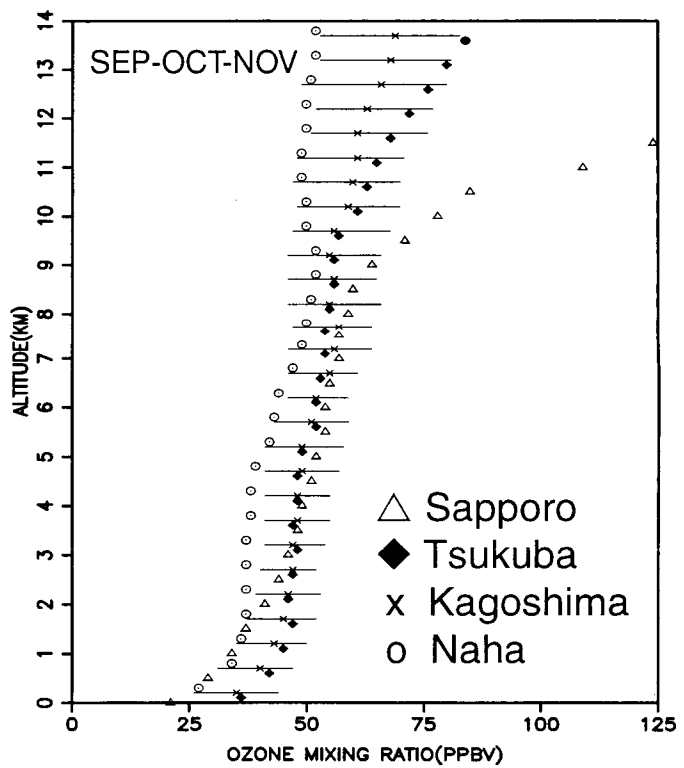
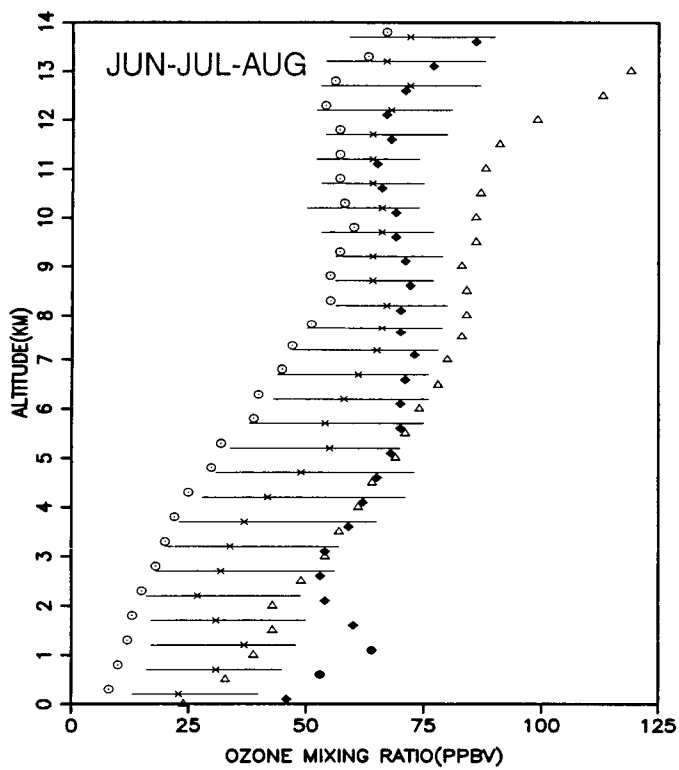
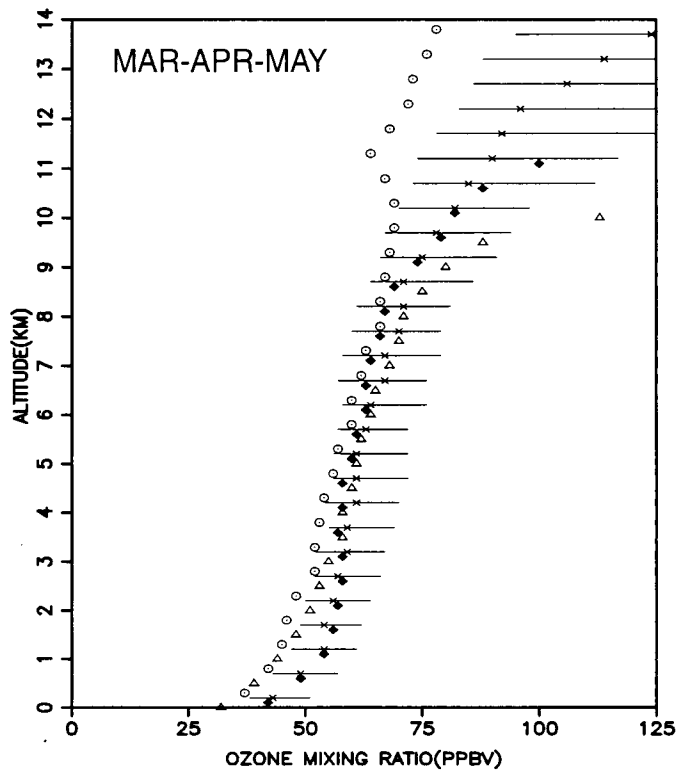
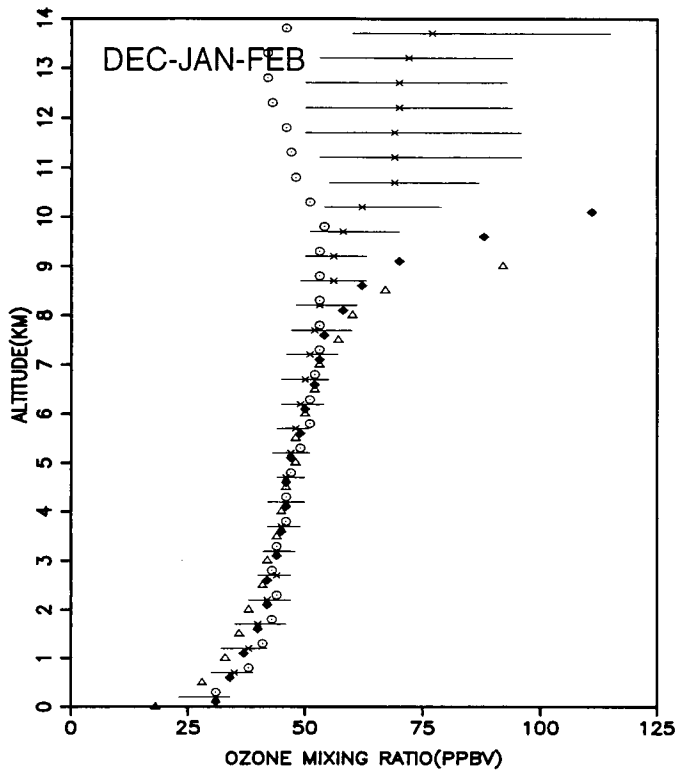


Figure 2: Average ozone vertical profiles by season at four Japanese stations.

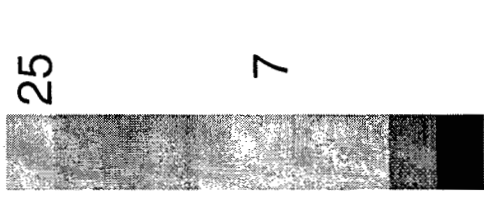
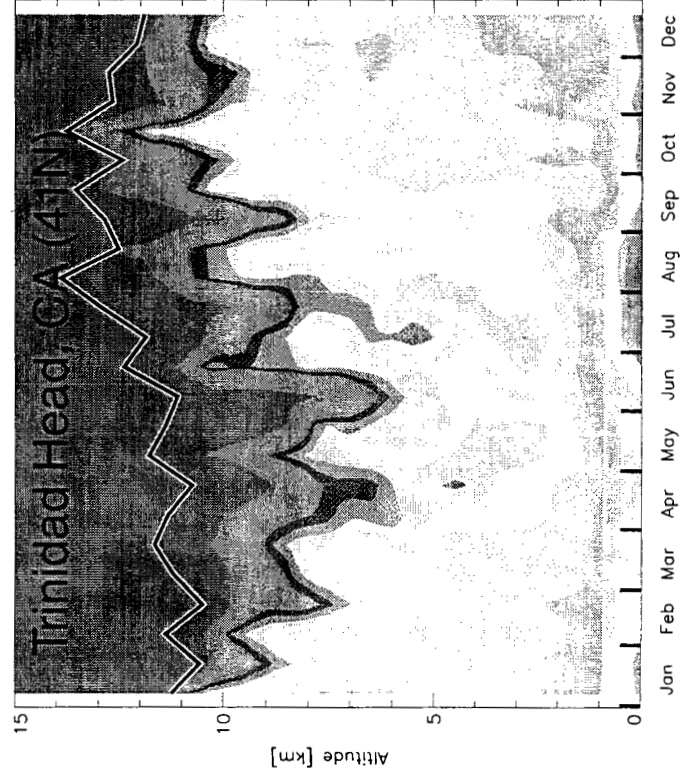
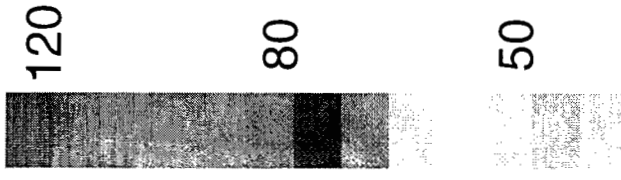
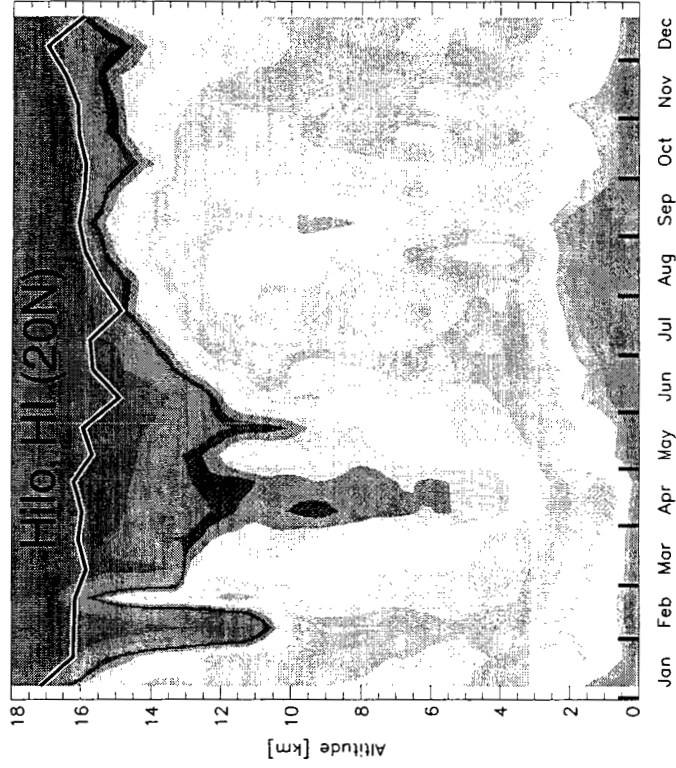
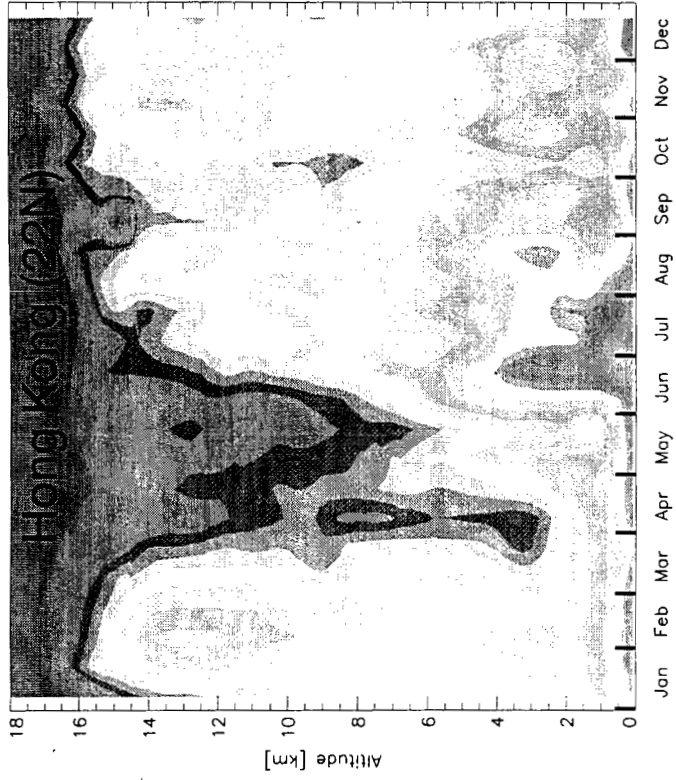


Figure 3: Average seasonal variation of the ozone mixing ratio at Hong Kong, Hilo, and Trinidad Head. Note the different altitude scale for Trinidad Head.

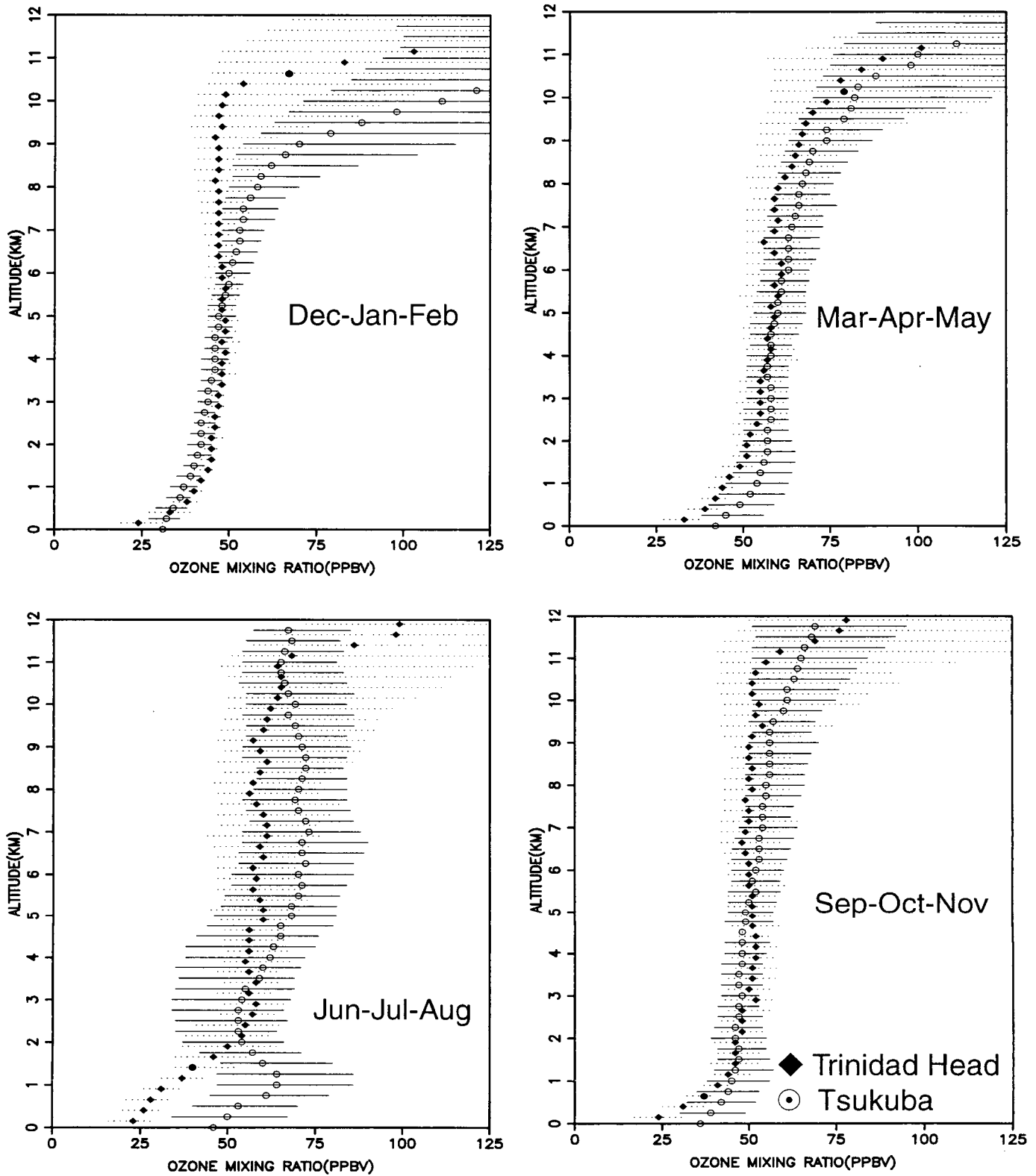


Figure 4: Comparison of the seasonal ozone profiles at Tsukua, Japan and Trinidad Head, California.

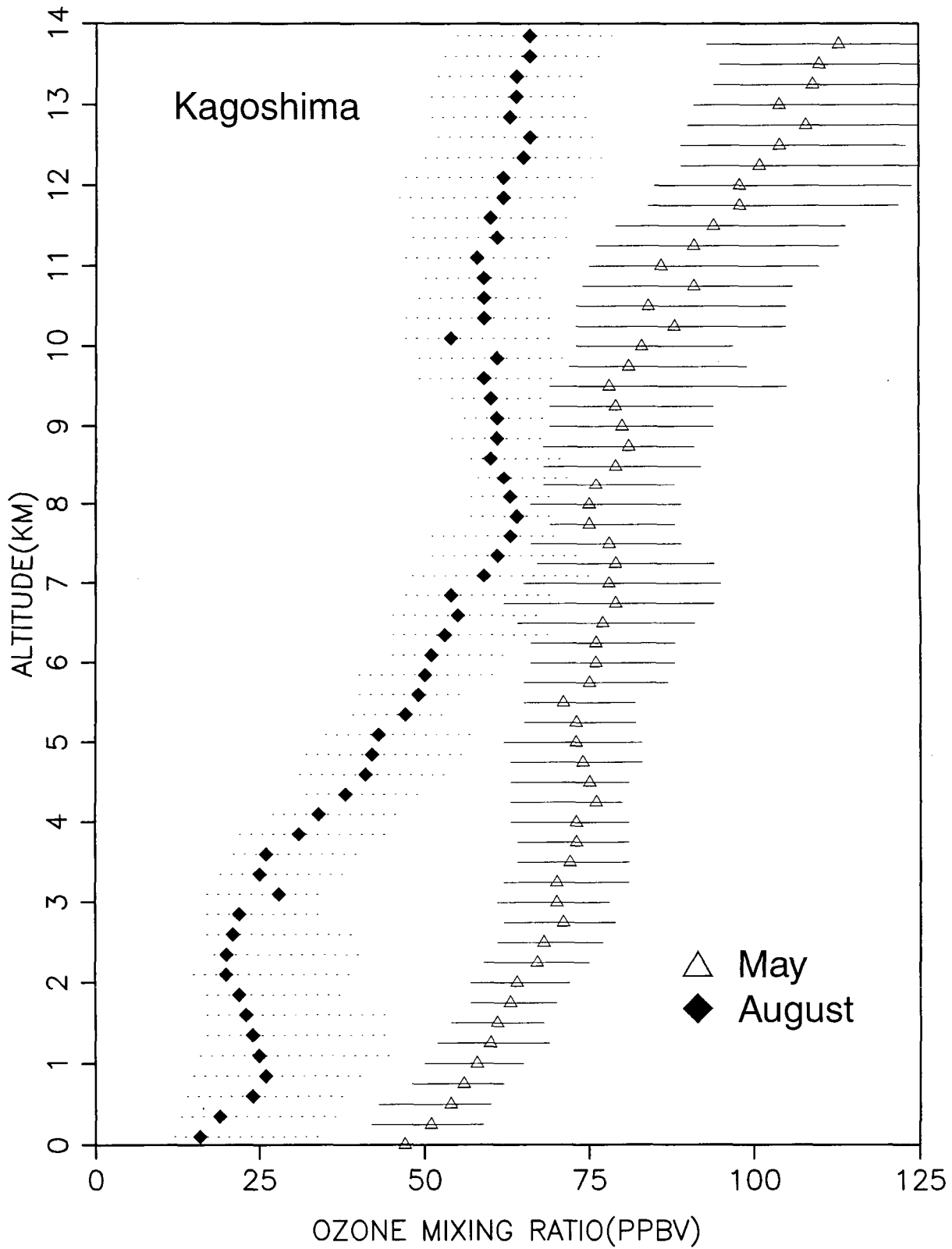


Figure 5: Median monthly tropospheric ozone mixing ratios for May and August for Kagoshima

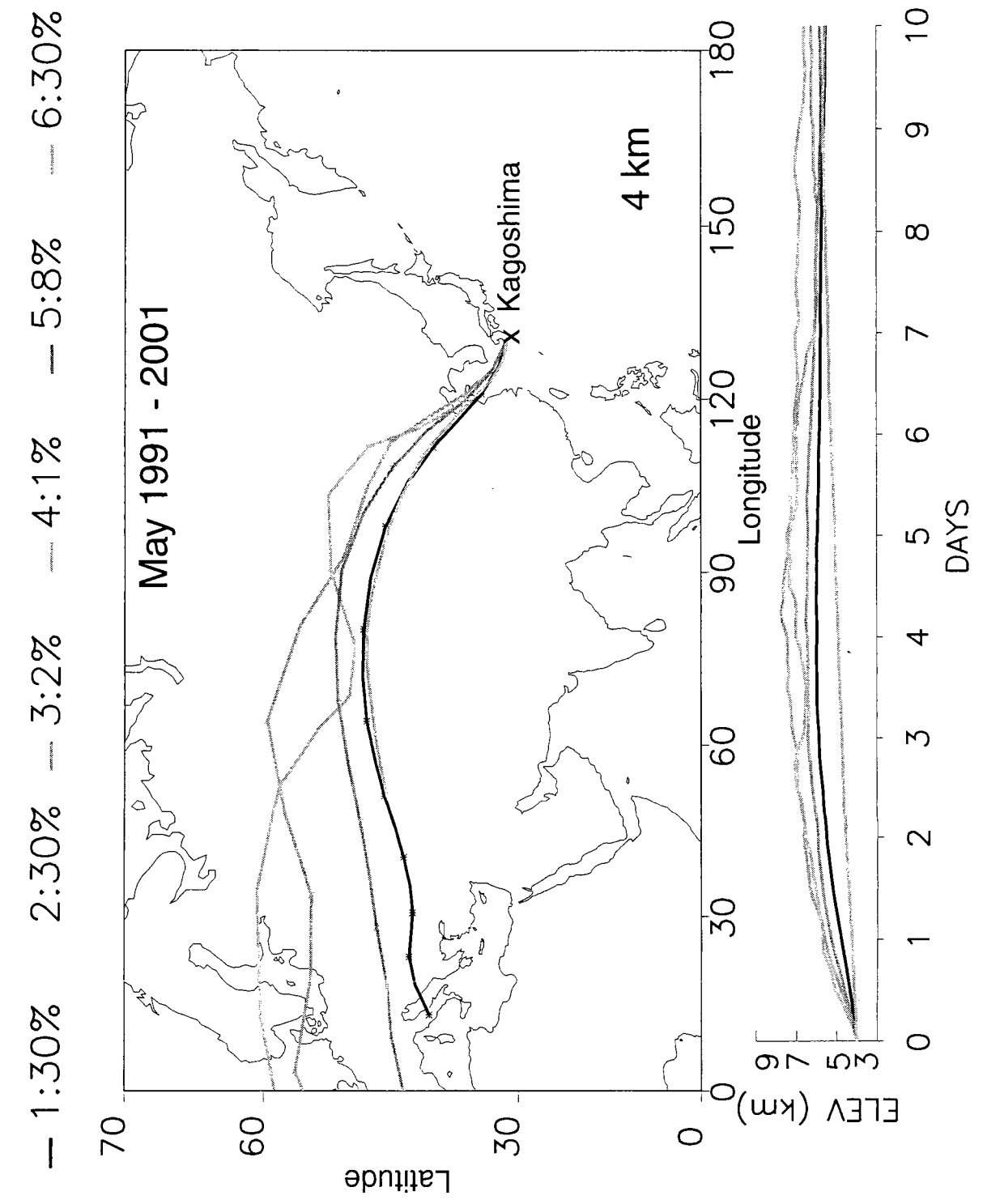


Figure 6a: Average air parcel trajectories arriving at 4km at Kagoshima for May

- 1:9%    2:33%    3:13%    4:25%    5:13%    6:7%

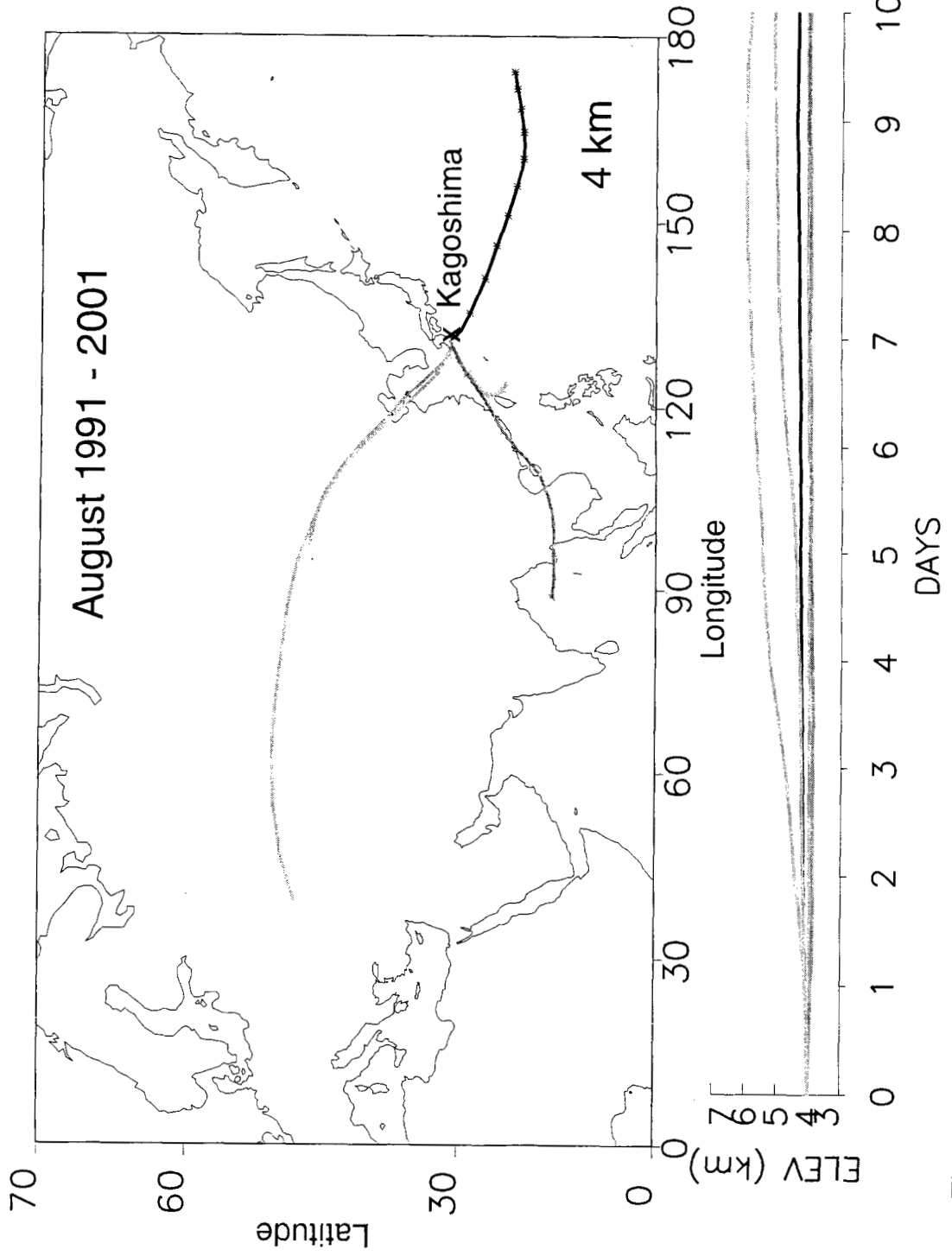


Figure 6b: Average air parcel trajectories arriving at 4km at Kagoshima for August

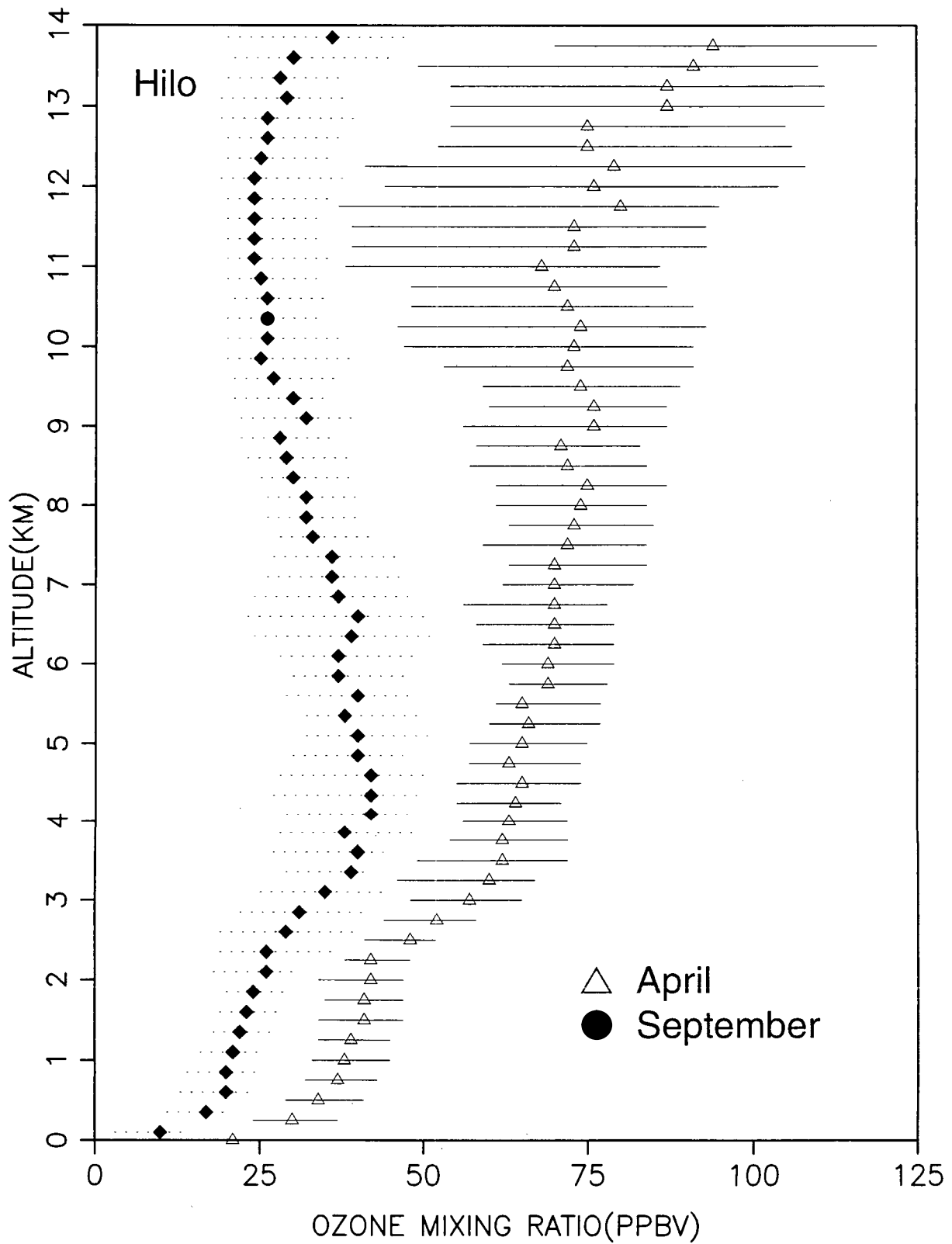


Figure 7: Median monthly tropospheric ozone mixing ratio for Hilo for April and September

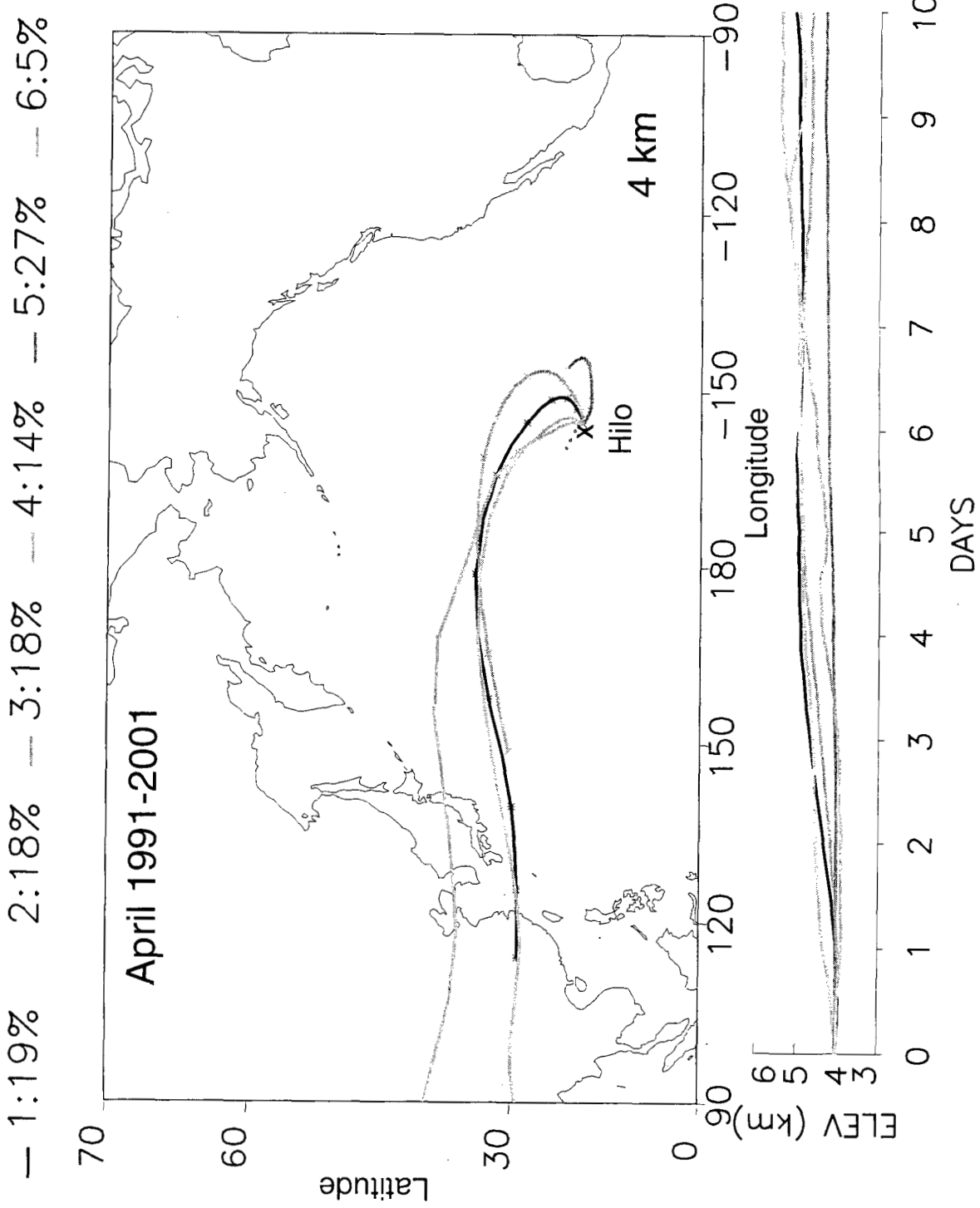


Figure 8a: Average air parcel trajectories arriving at 4 km for Hilo for April

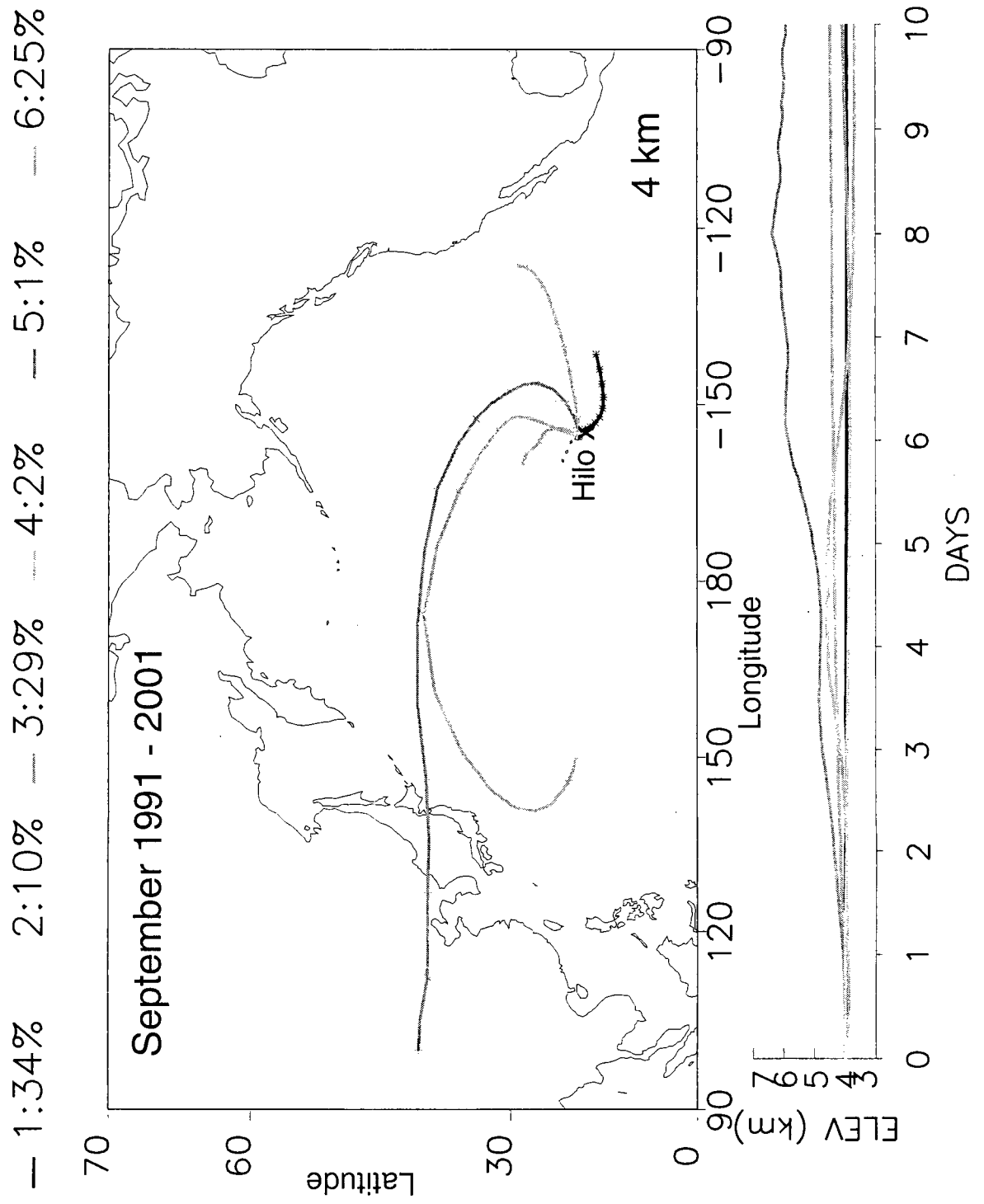


Figure 8b: Average air parcel trajectories arriving at 4 km for Hilo for September

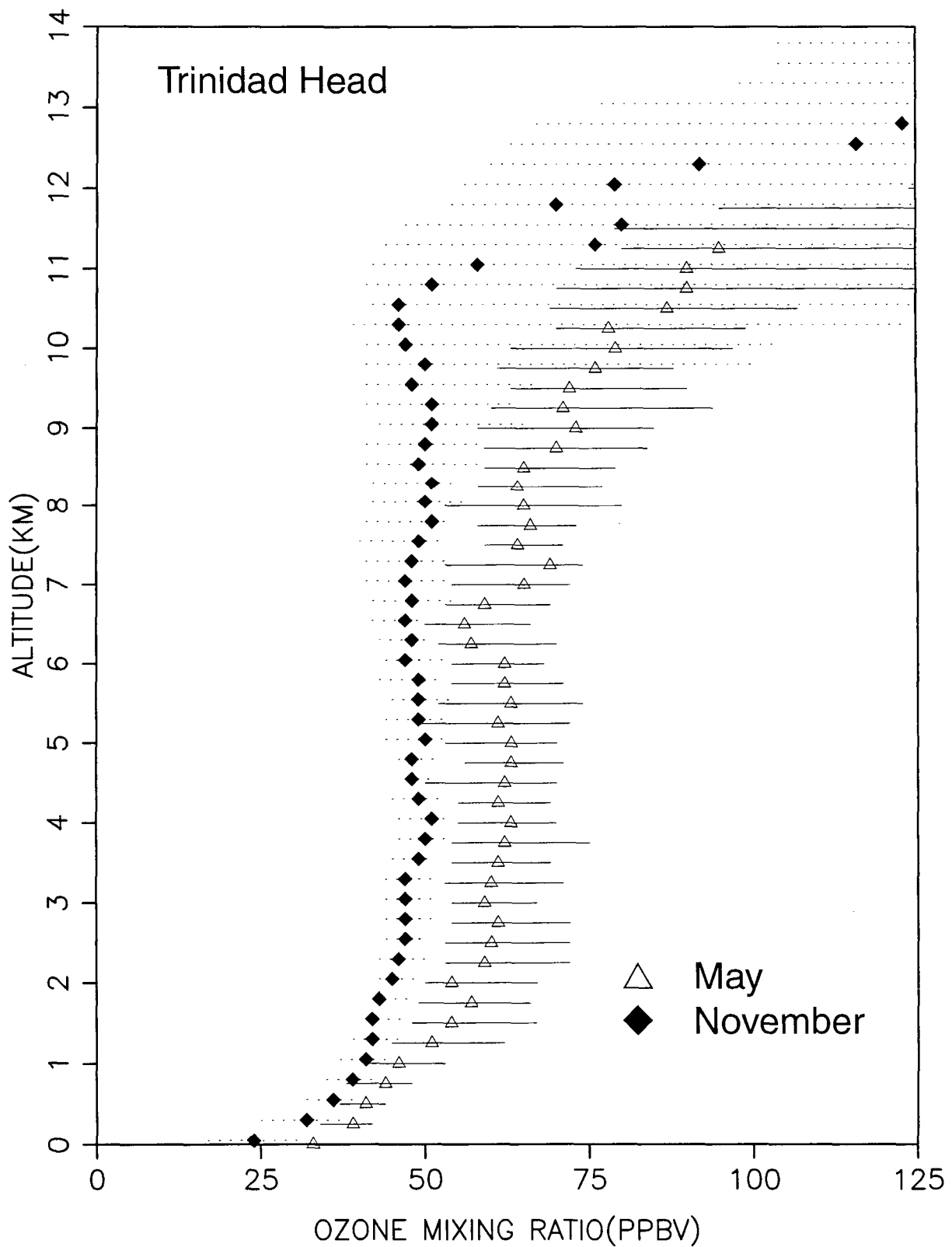


Figure 9: Median monthly tropospheric ozone mixing ratio for May and November for Trinidad Head, California

— 1:25%    2:24%    3:21%    4:22%    5:1%    6:7%

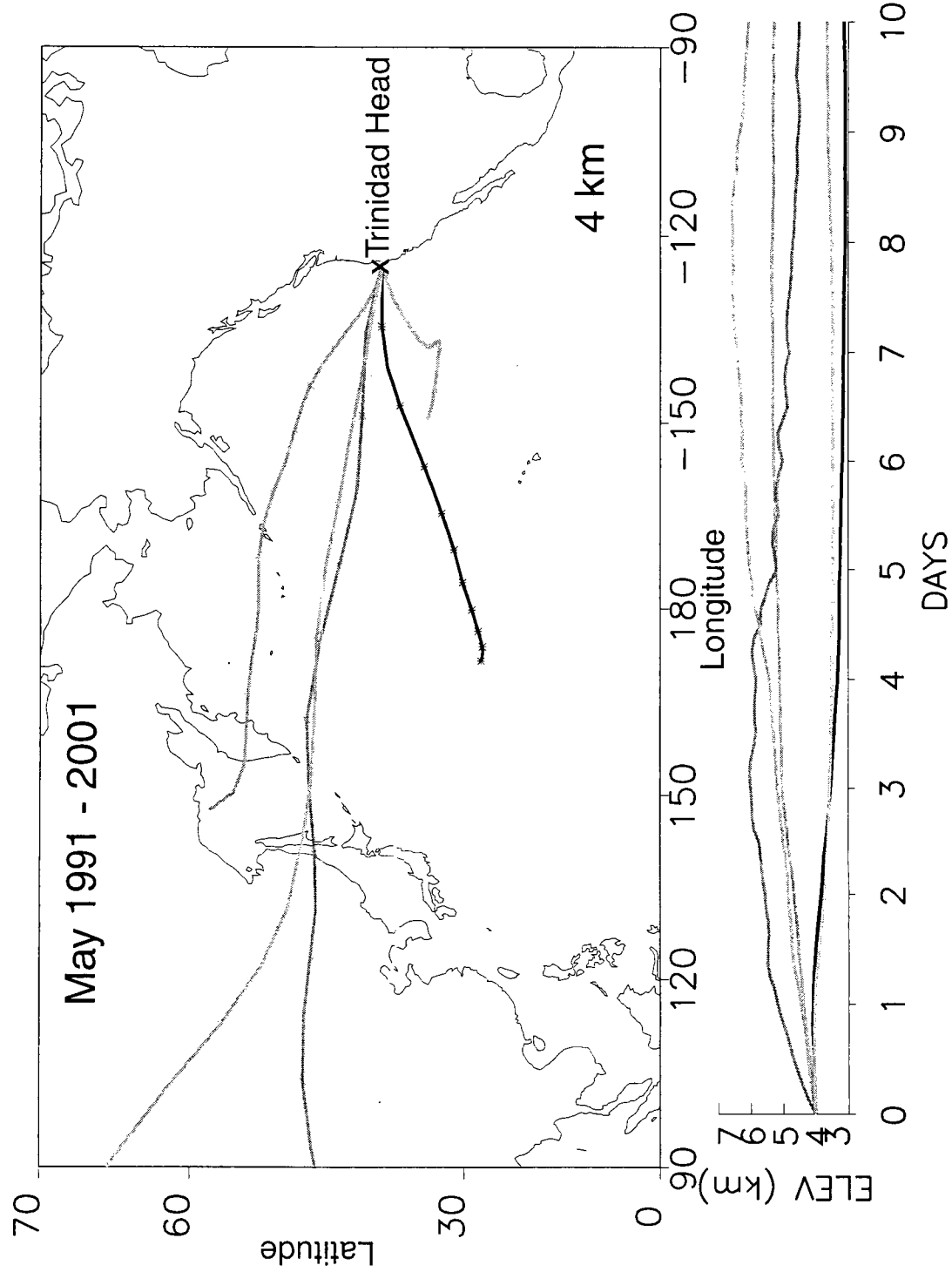


Figure 10a: Average air parcel trajectories arriving at 4 km at Trinidad Head for May

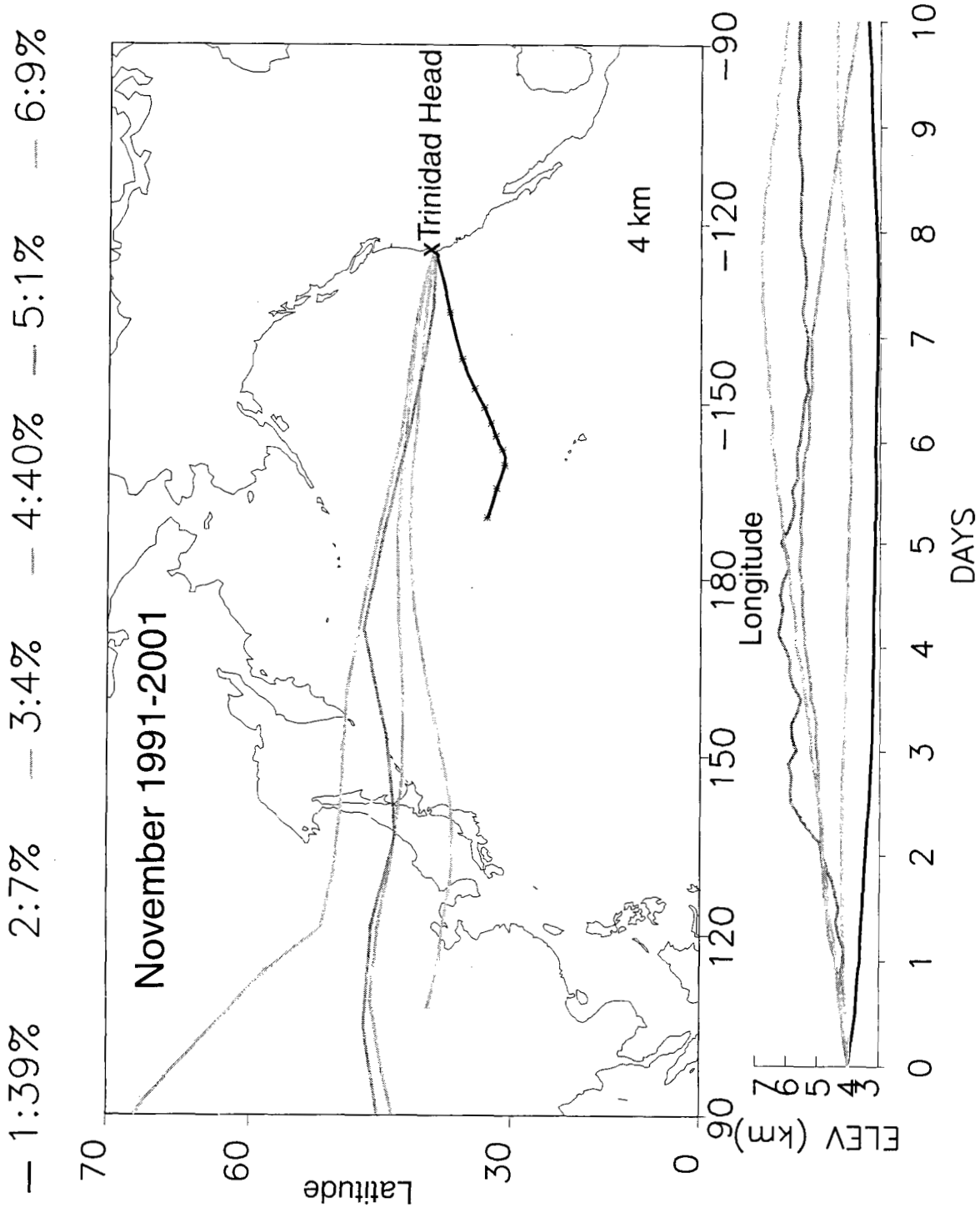


Figure 10b: Average air parcel trajectories arriving at 4 km at Trinidad Head for November

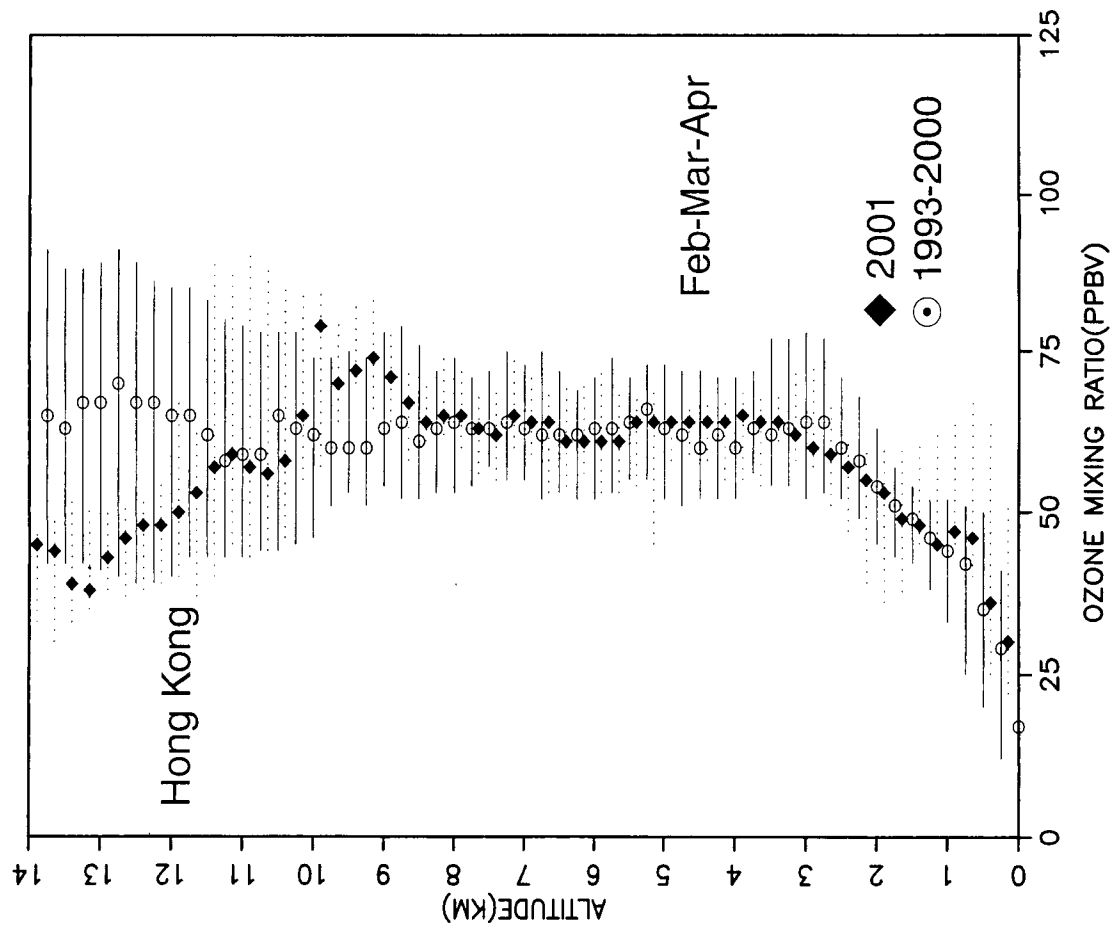
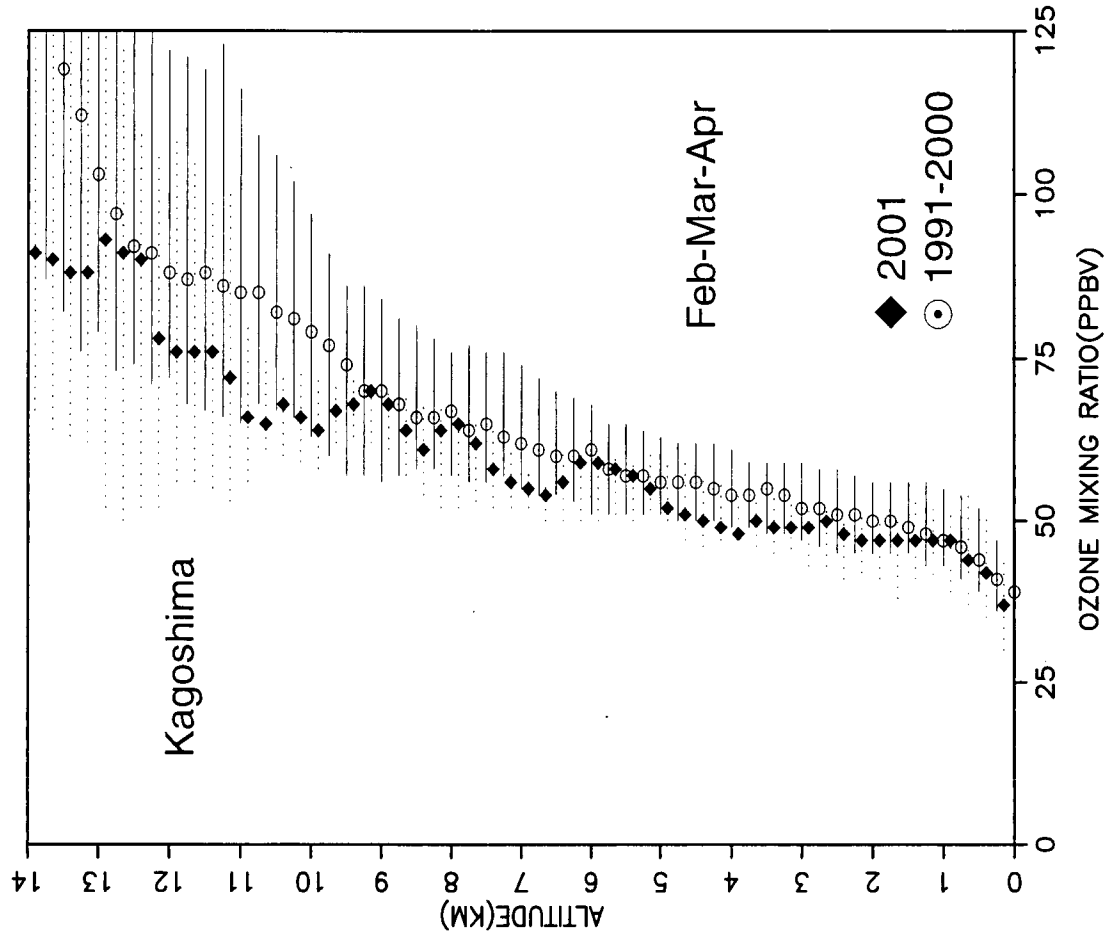


Figure 11: Comparison of the February-March-April 2001 median ozone mixing ratios with the long-term average for Hong Kong and Kagoshima

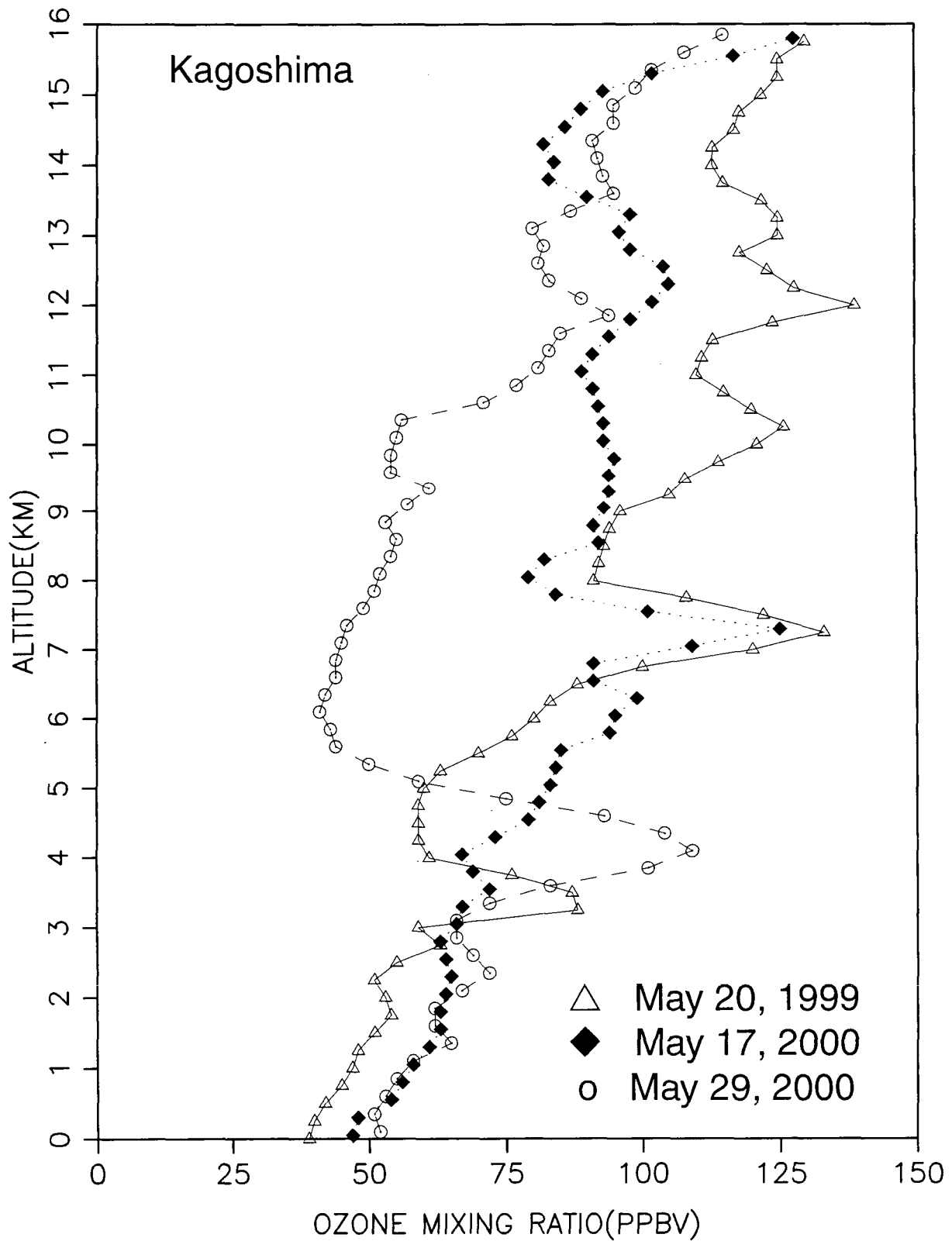


Figure 12: Profiles of ozone mixing ratio at Kagoshima on May 20, 1999, May 17, 2000, and May 29, 2000

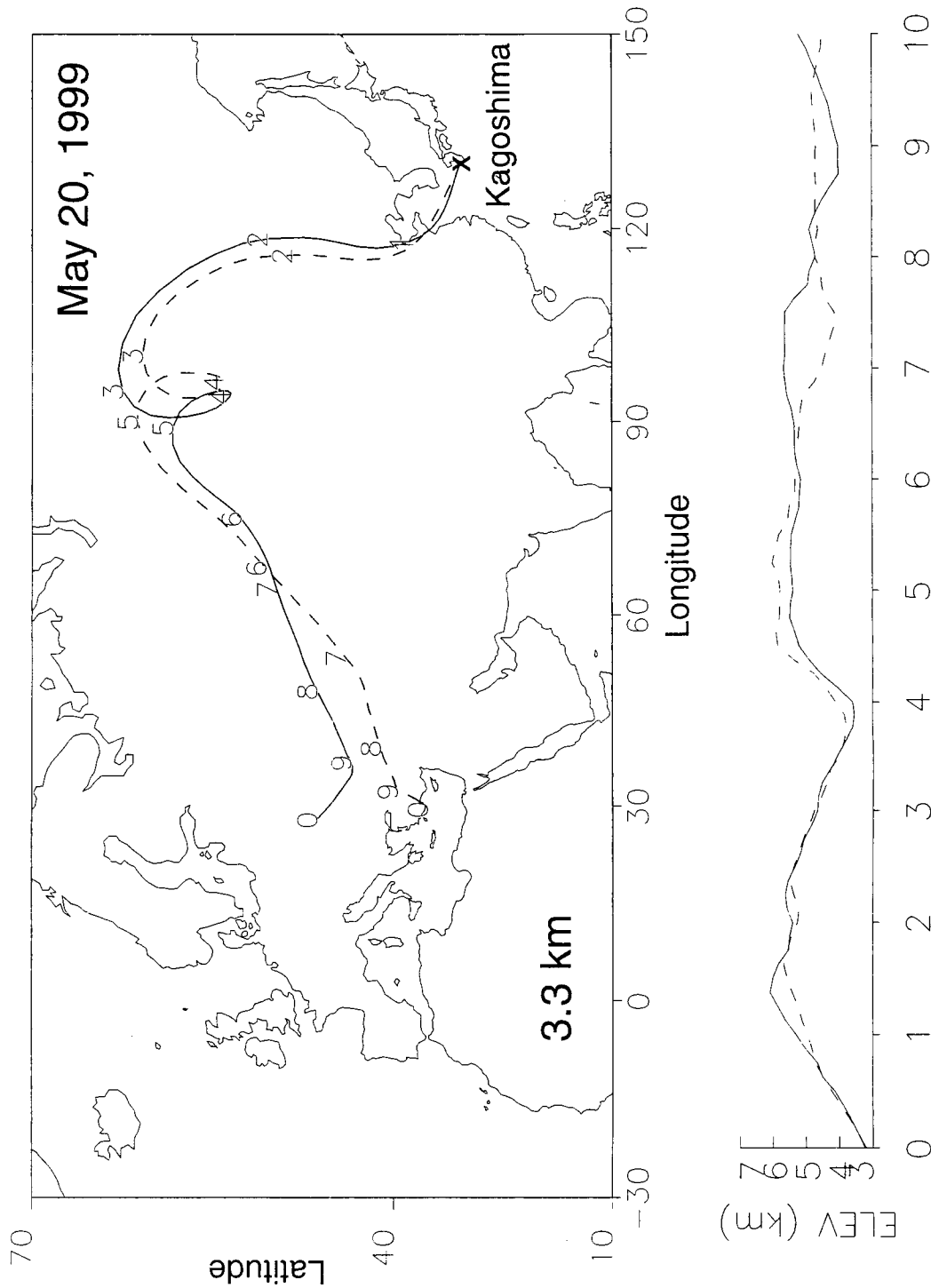


Figure 13: Isentropic, 10-day back trajectory to Kagoshima arriving on May 20, 1999 at 3.3 km

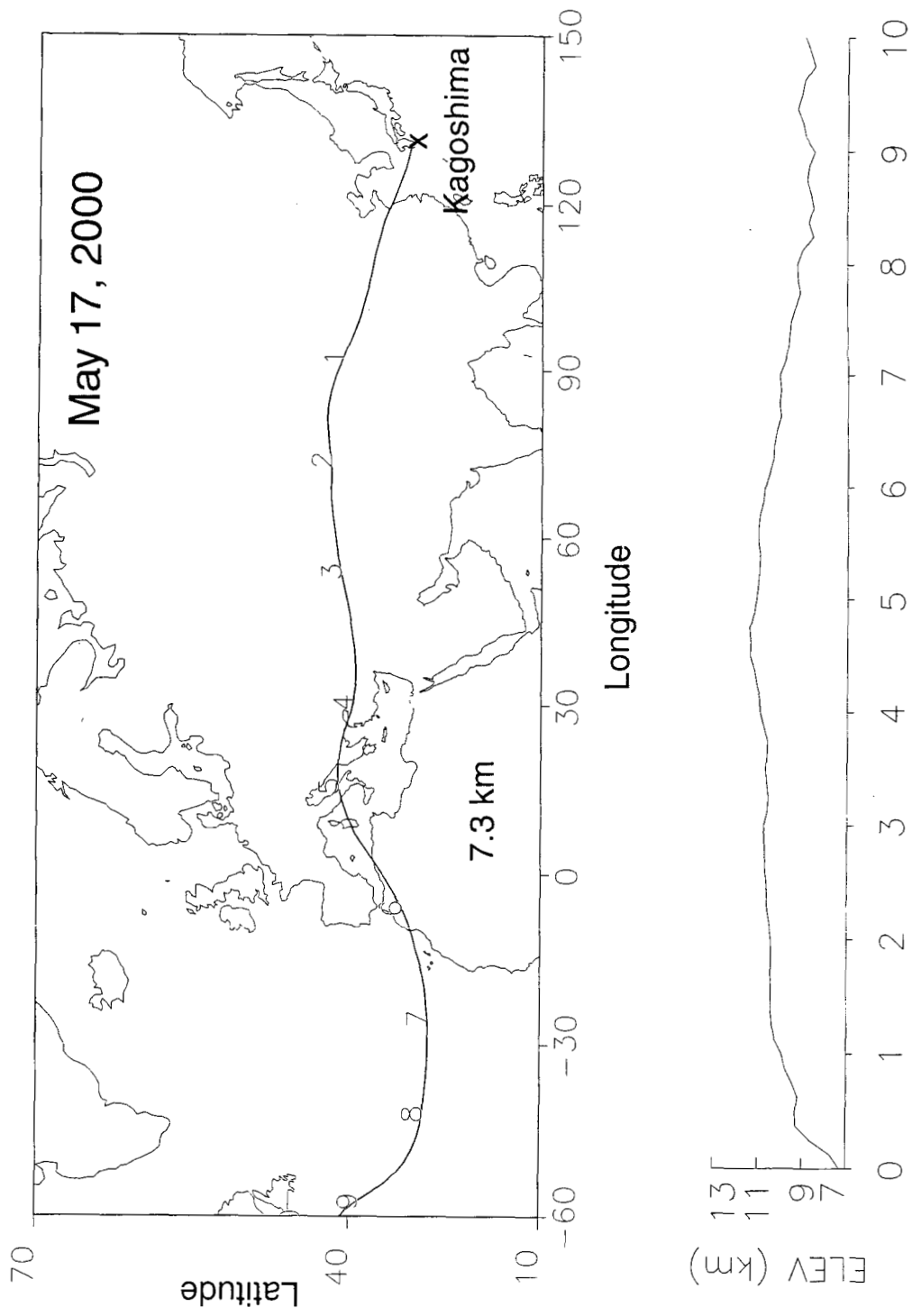


Figure 14: Insentropic, 10-day back trajectory to Kagoshima arriving on May 17, 2000 at 7.3 km at 1800 GMT

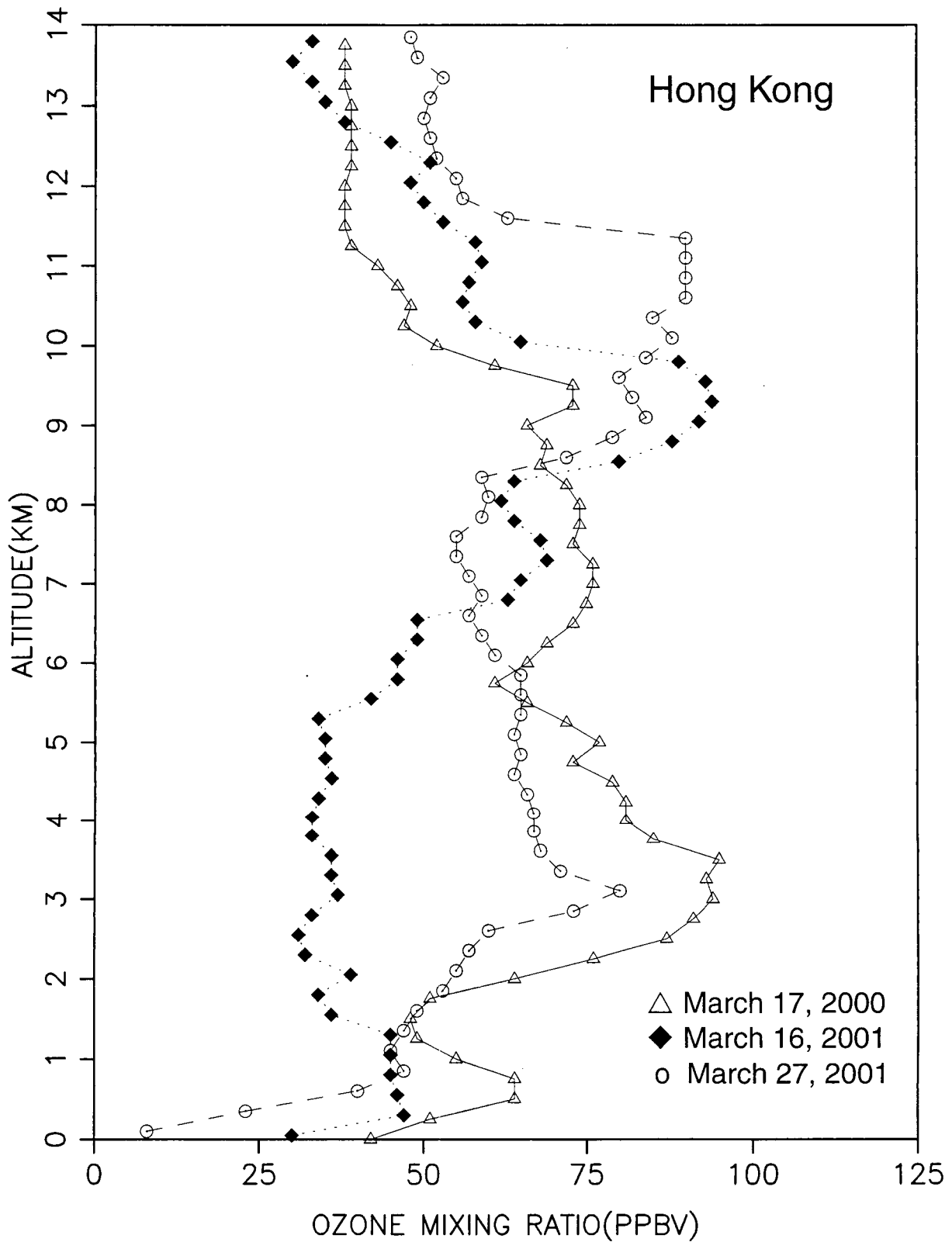


Figure 15: Profiles of ozone mixing ratio at Hong Kong on March 17, 2000, March 16, 2001, and March 27, 2001

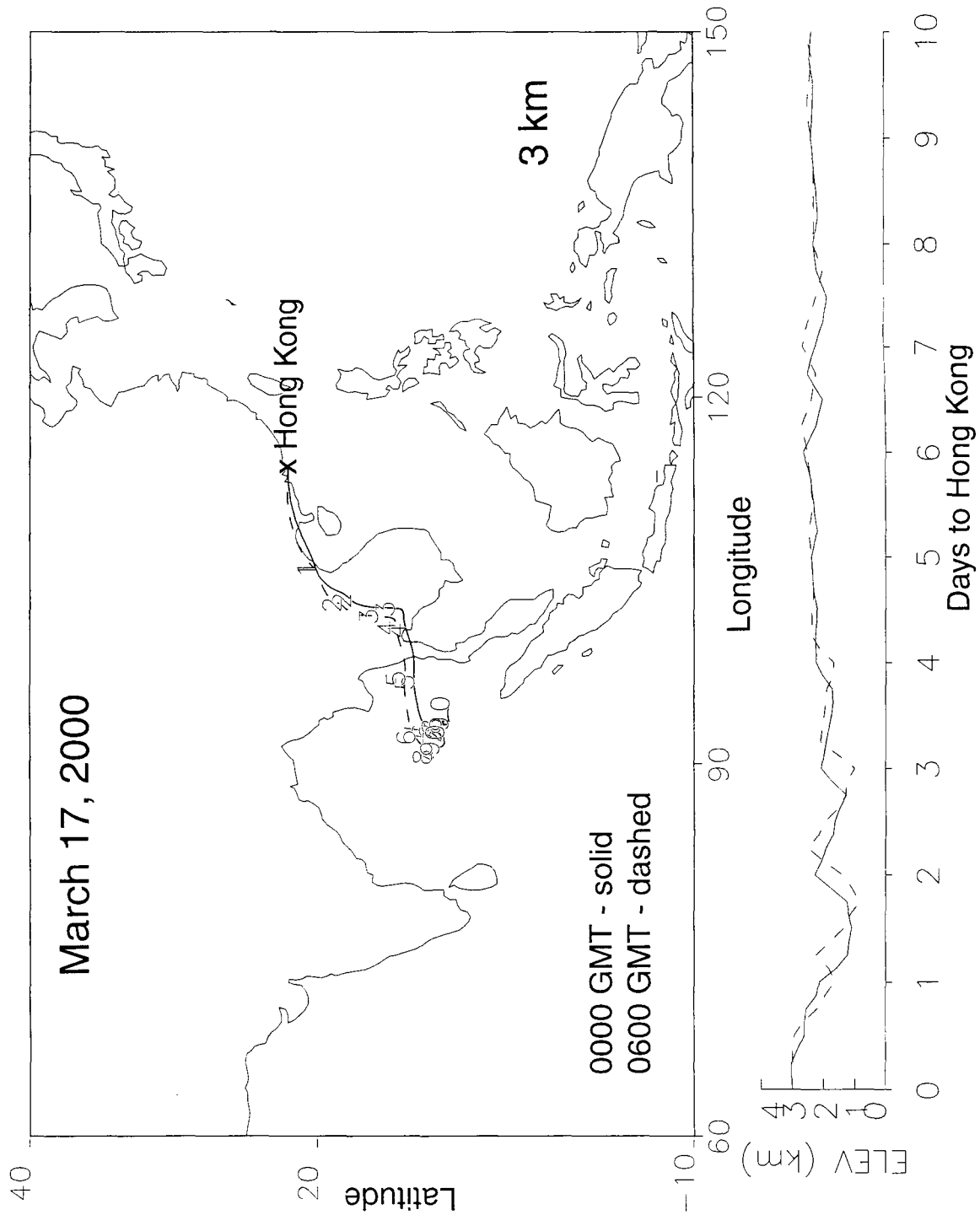


Figure 16: Inseotropic, 10-day back trajectory to Hong Kong arriving on March 17, 2000 at 3 km

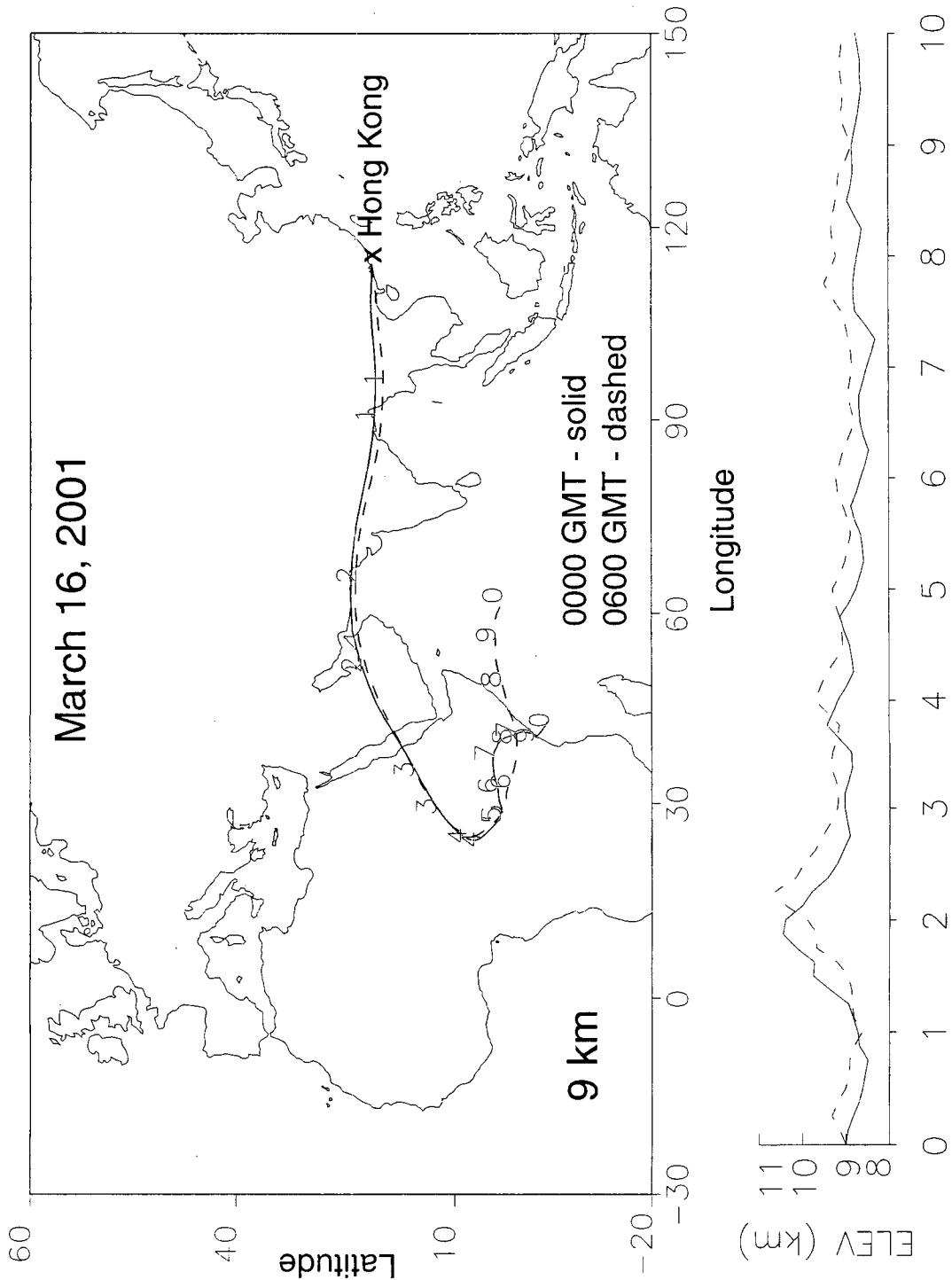


Figure 17: Inseotropic, 10-day back trajectory to Hong Kong arriving on March 17, 2000 at 9 km

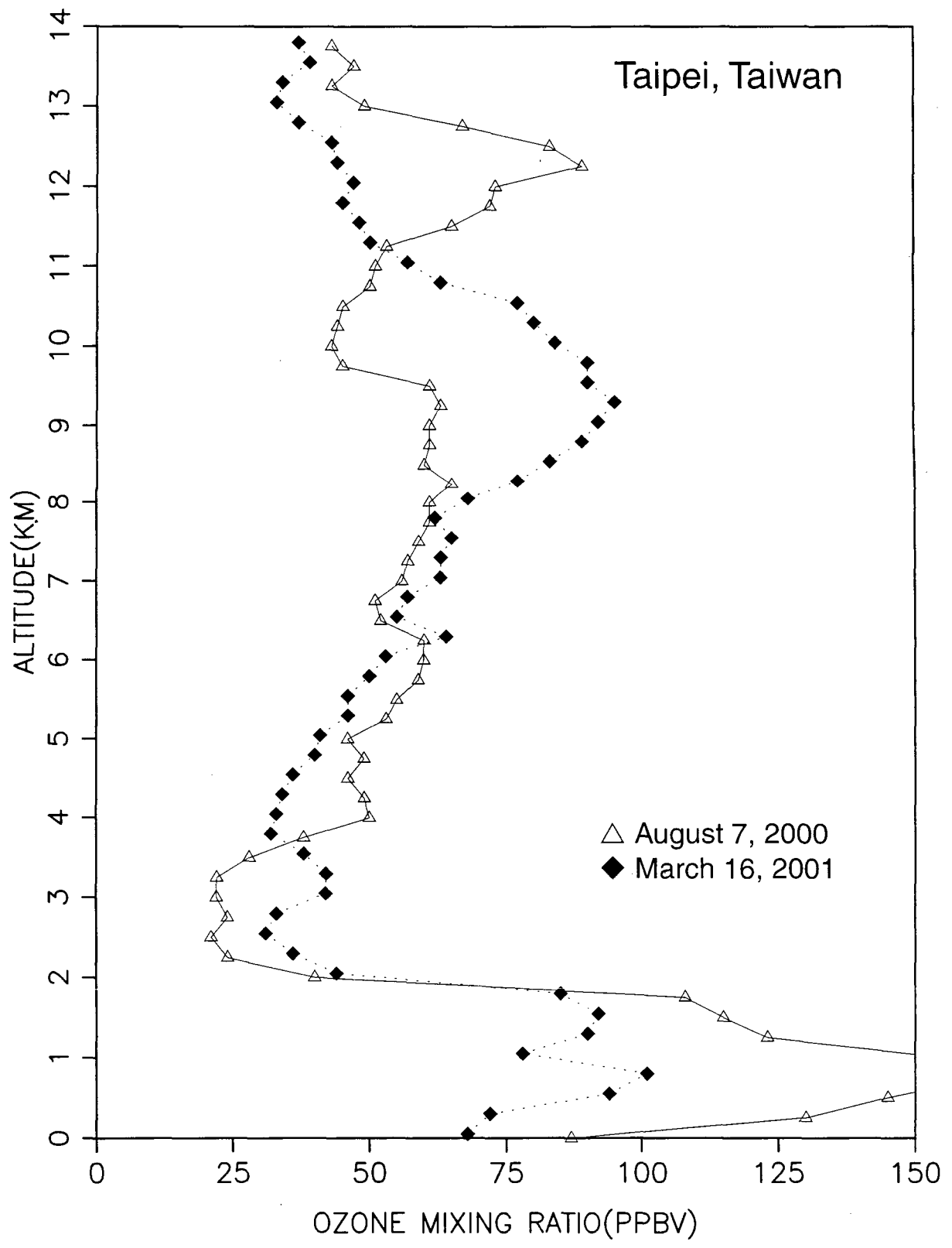


Figure 18: Profiles of ozone mixing ratio at Taipei on August 7, 2000 and March 16, 2001

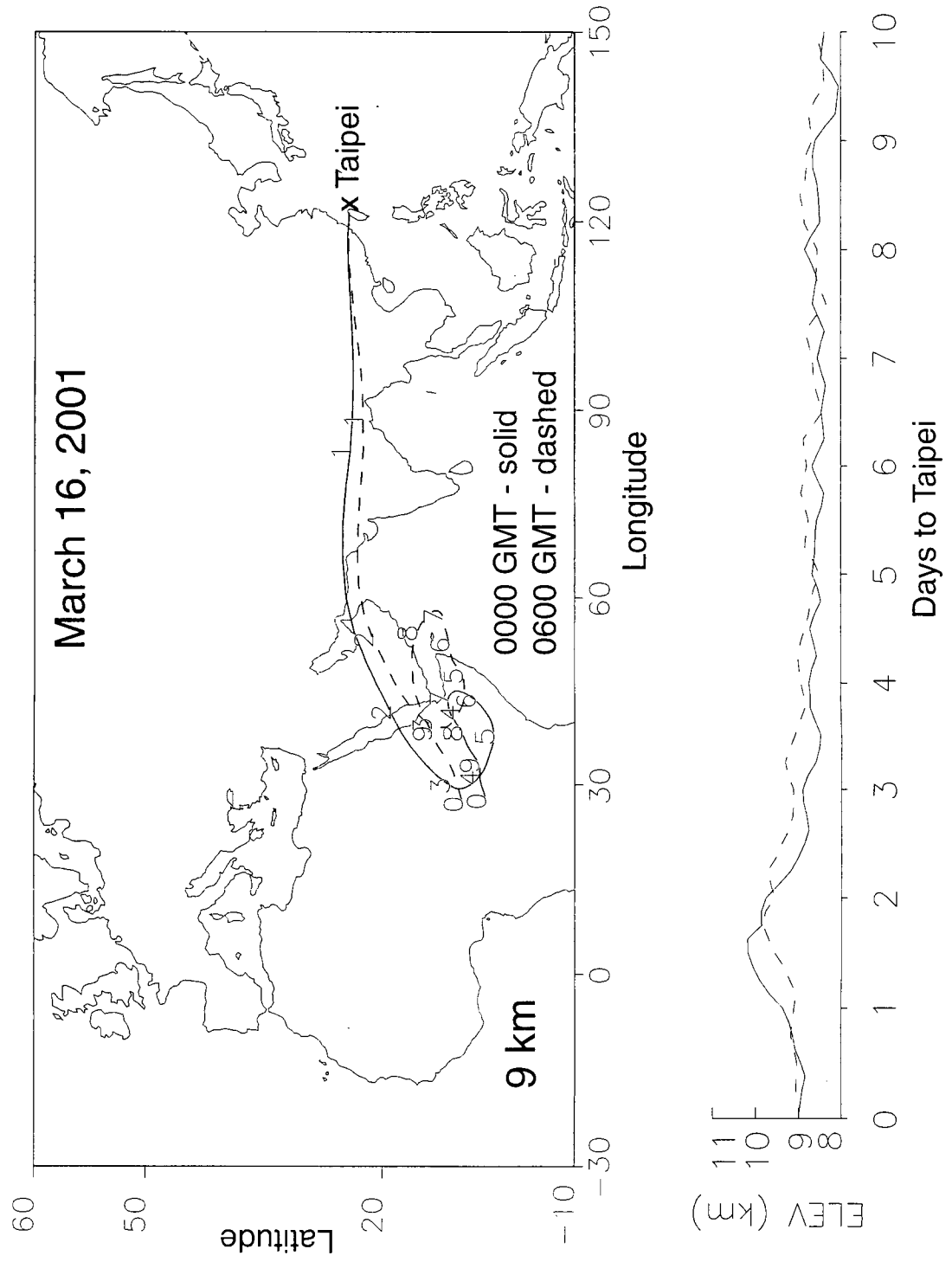


Figure 19: Isentropic, 10-day back trajectory to Taipei arriving on March 16, 2001 at 9 km

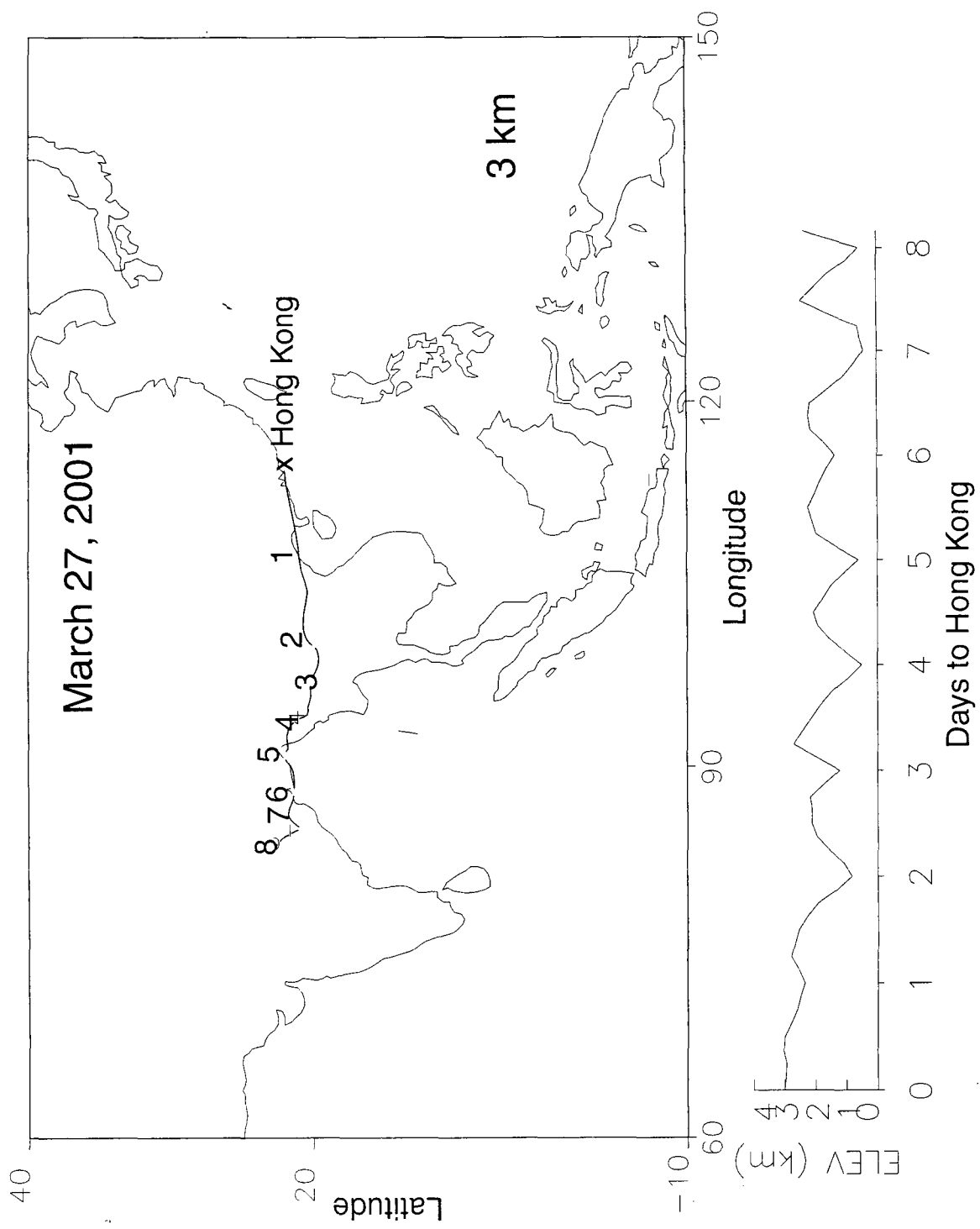


Figure 20a: Isentropic, 10-day back trajectory to Hong Kong arriving on March 27, 2001 at 3 km

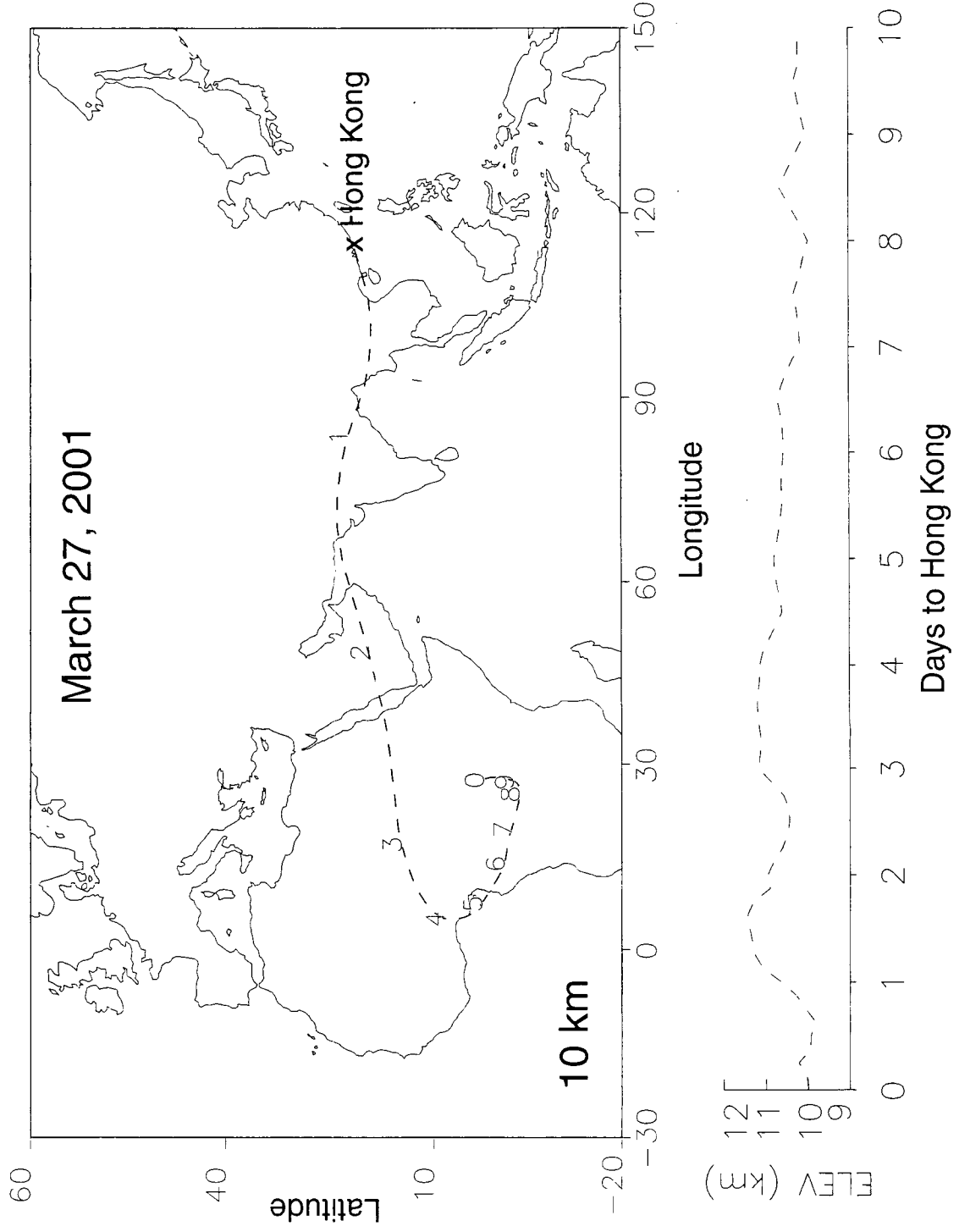


Figure 20b: Inseotropic, 10-day back trajectory to Hong Kong arriving on March 27, 2001 at 10 km



Figure 21: Fire counts for March 2001 from the European Space Agency World Fire Atlas compiled from observations made by the ASTR instrument on the ERS-2 satellite. The fire locations are the red dots.

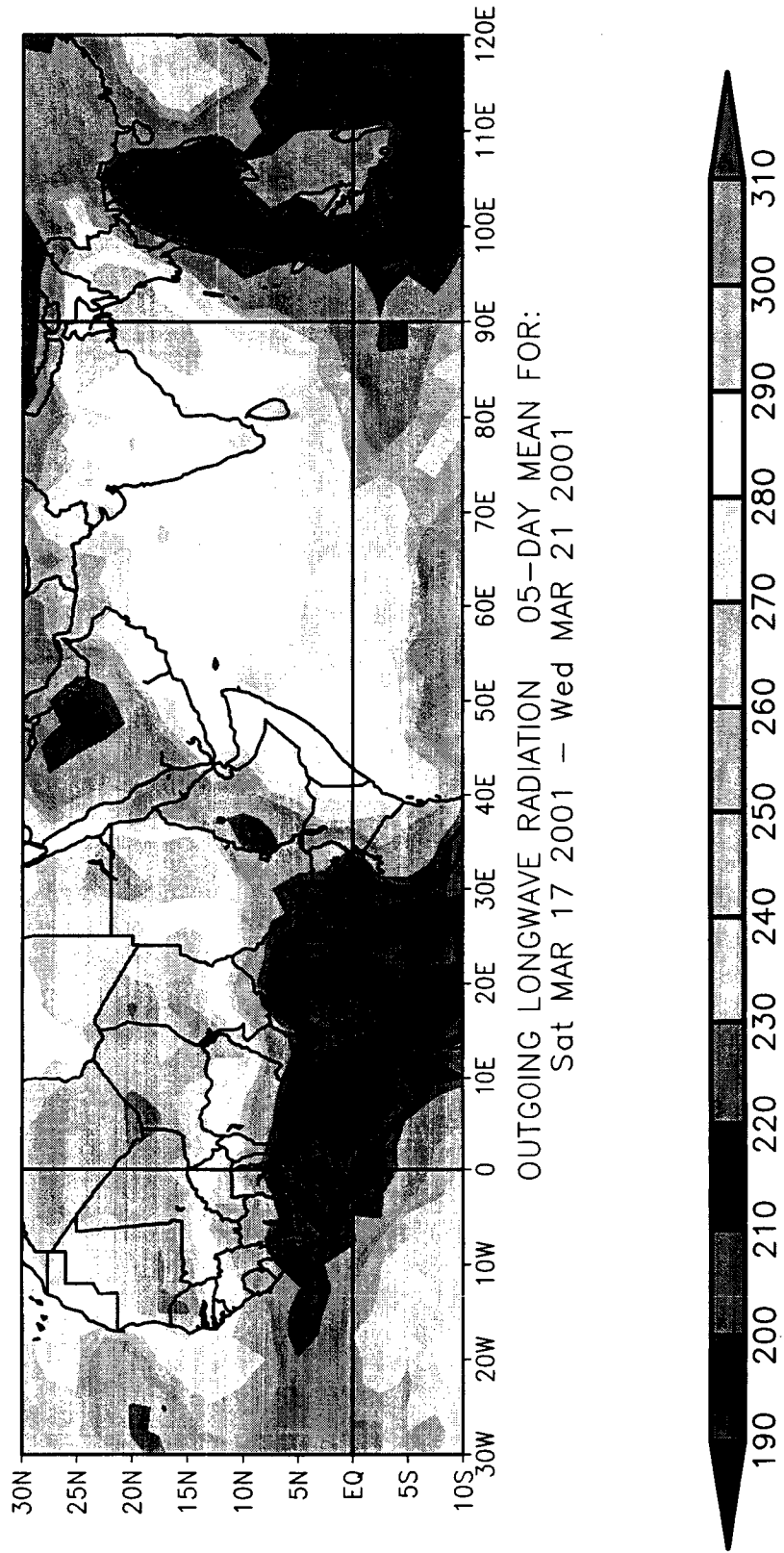


Figure 22: Outgoing Longwave Radiation (OLR) data averaged for the five day period March 17-21, 2001. Low values of OLR are indicative of thick cloudiness associated with convected activity. Data provided by the NOAA Climate Diagnostics Center.

***Tropical Tropospheric Ozone, EP/TOMS  
Mar. 22, 01 - Mar. 24, 01***

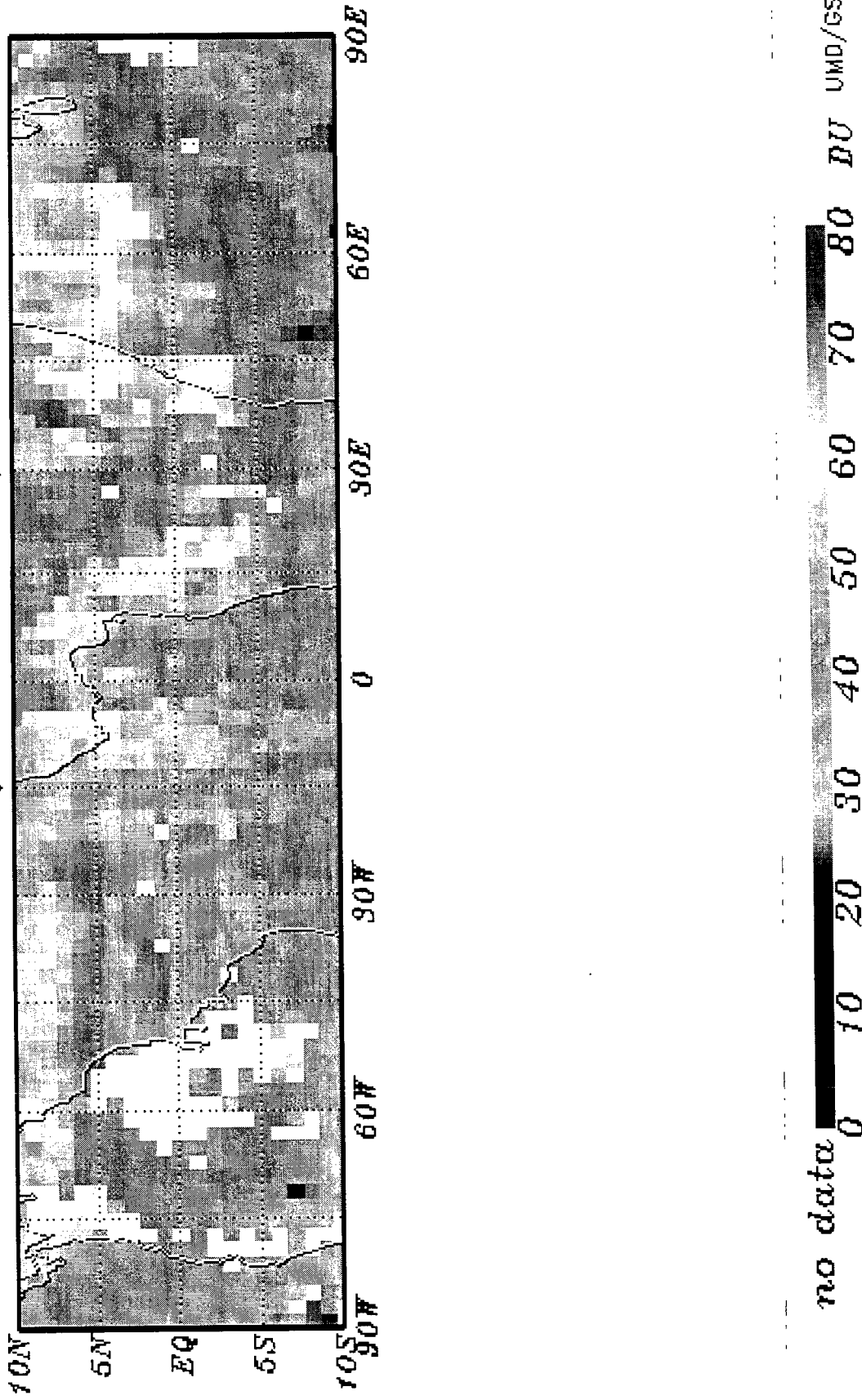


Figure 23: Tropical Tropospheric Ozone (TTO) derived from the Earth Probe TOMS

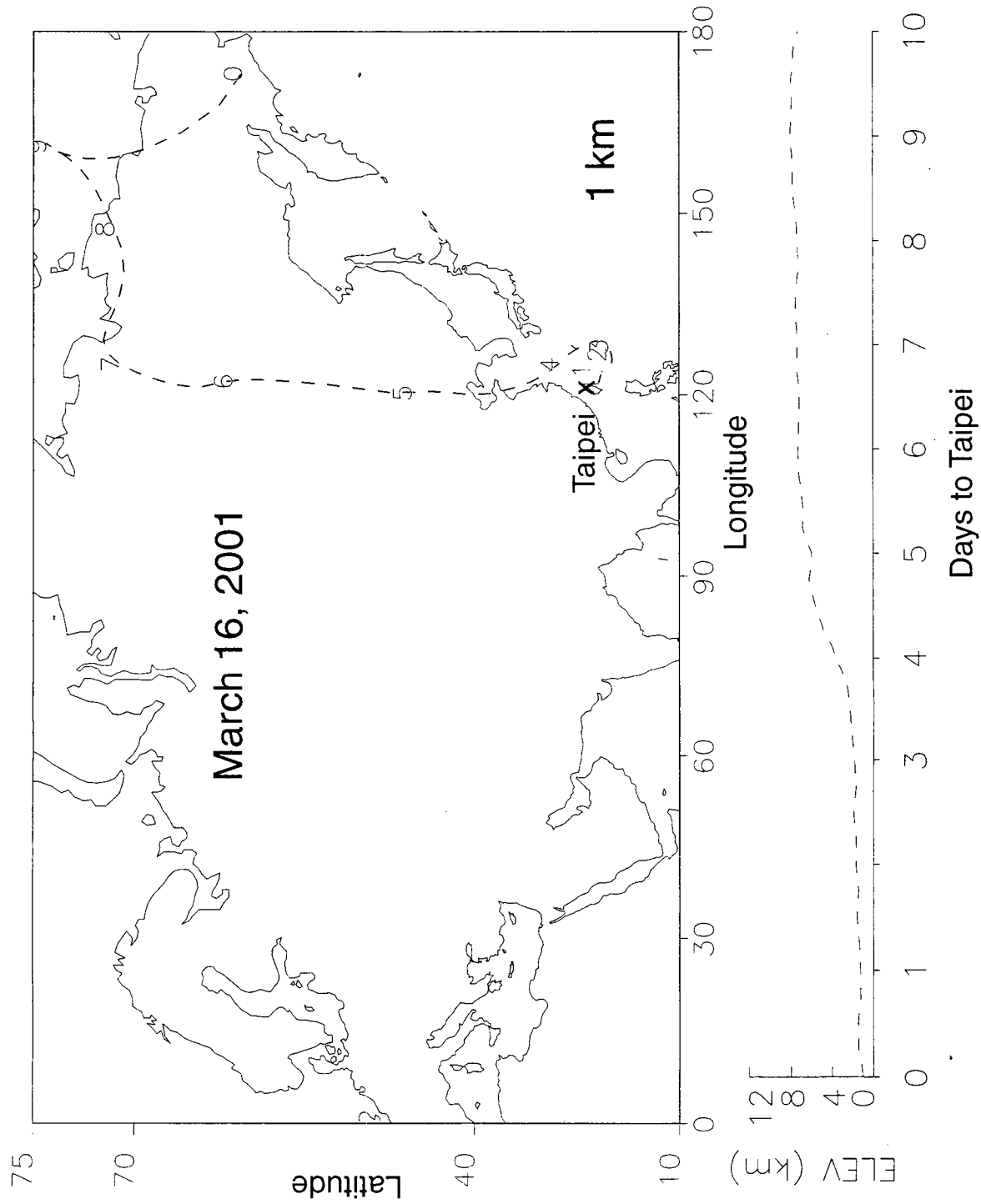


Figure 24: Isentropic, 10-day back trajectory to Taipei arriving on March 16, 2001 at 1 km.

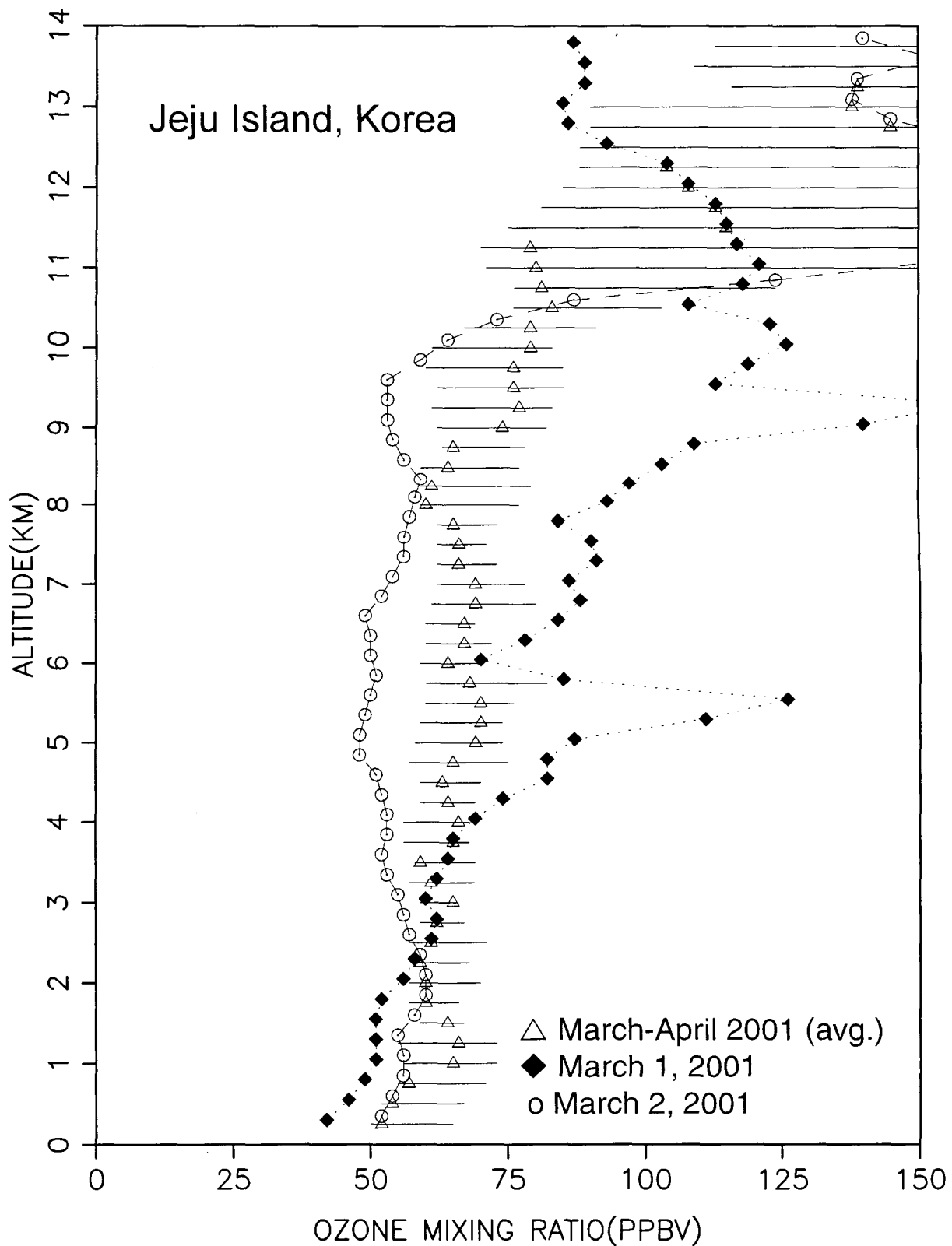


Figure 25: Profiles of ozone mixing ratio at Jeju Island on March 1, 2001 and March 2, 2001. The average profile for the eight soundings during March and April 2001 is also shown.

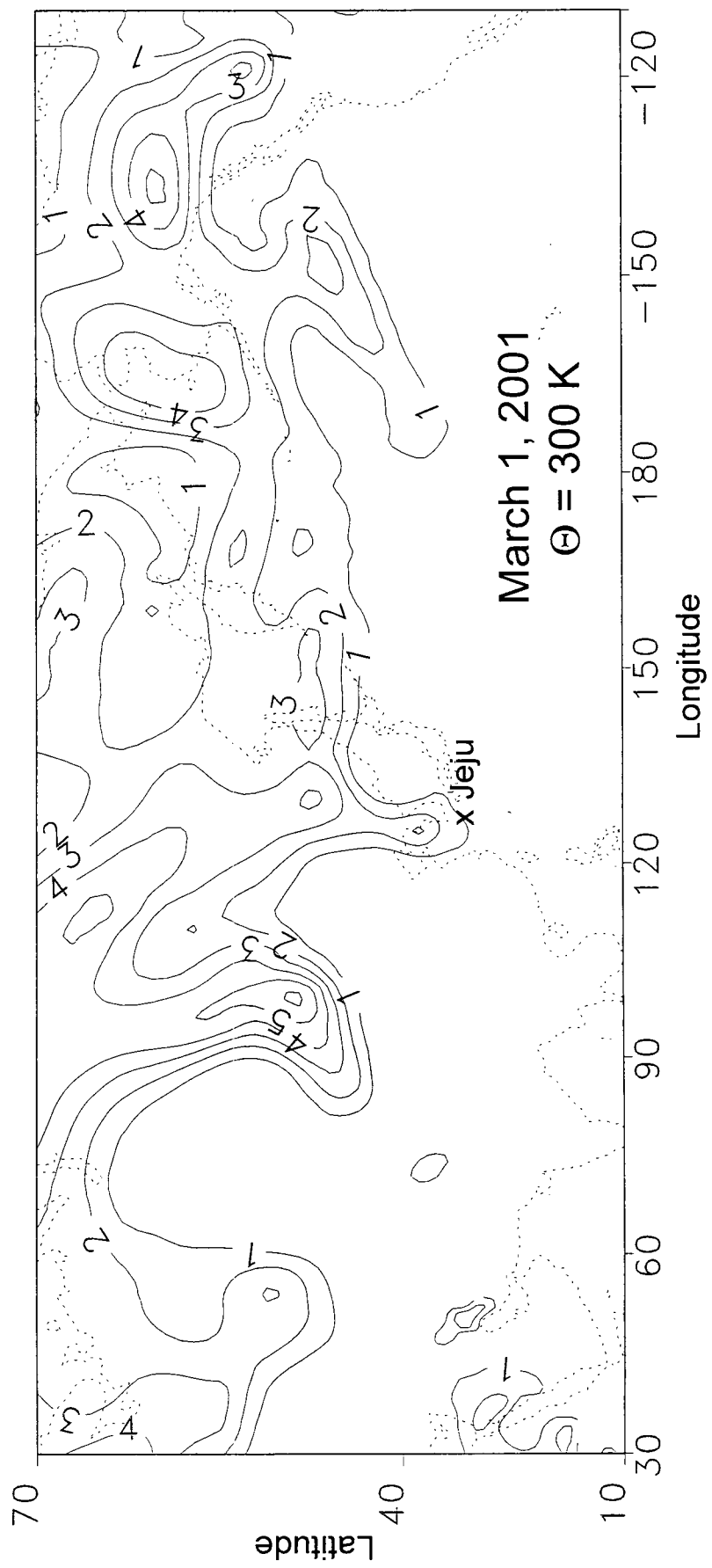


Figure 26a: Potential vorticity on March 1, 2001 at 0600 GMT on the 300 K potential temperature surface.

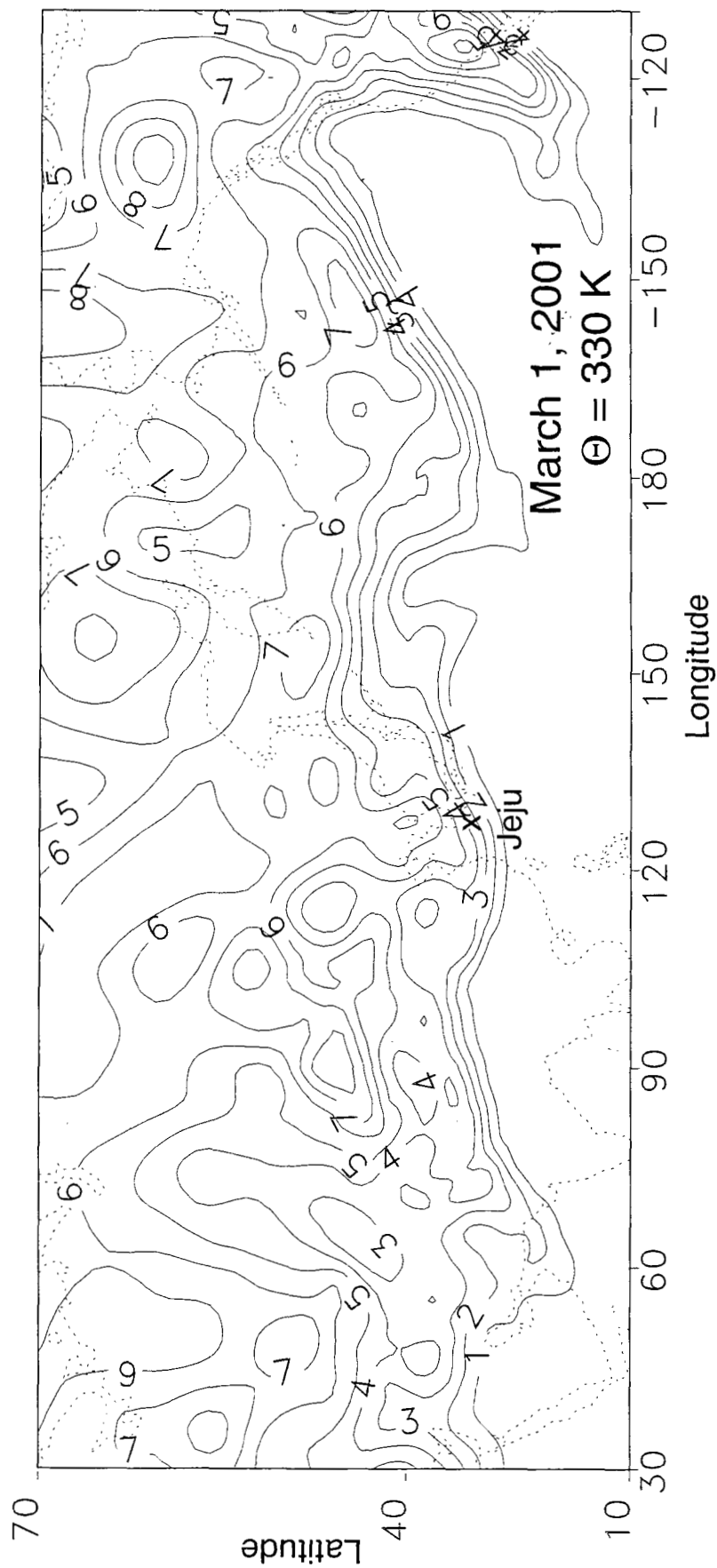


Figure 26b: Potential vorticity on March 1, 2001 at 0600 GMT on the 330 K potential temperature surface

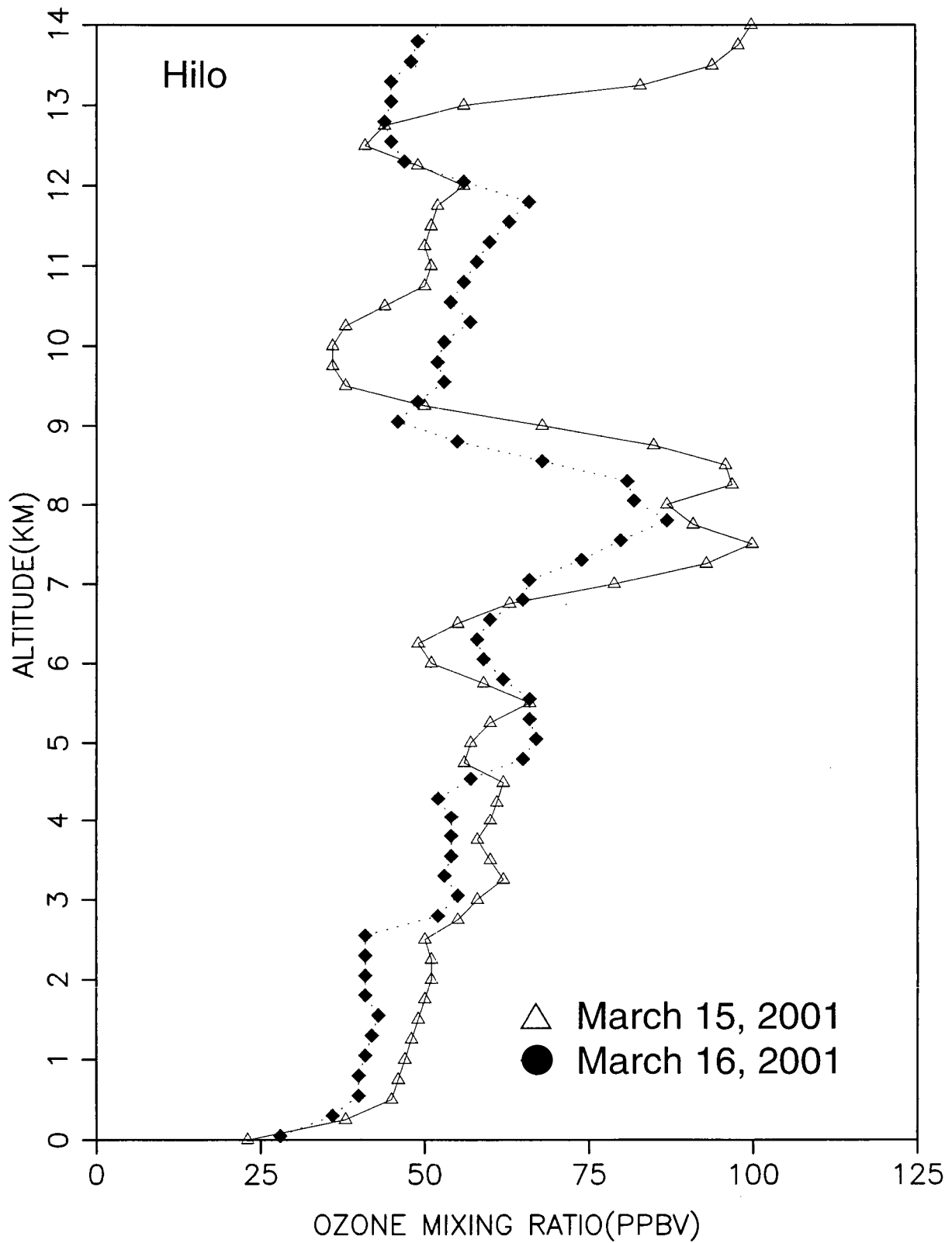


Figure 27: Profiles of ozone mixing ratio at Hilo on March 15 and 16, 2001.

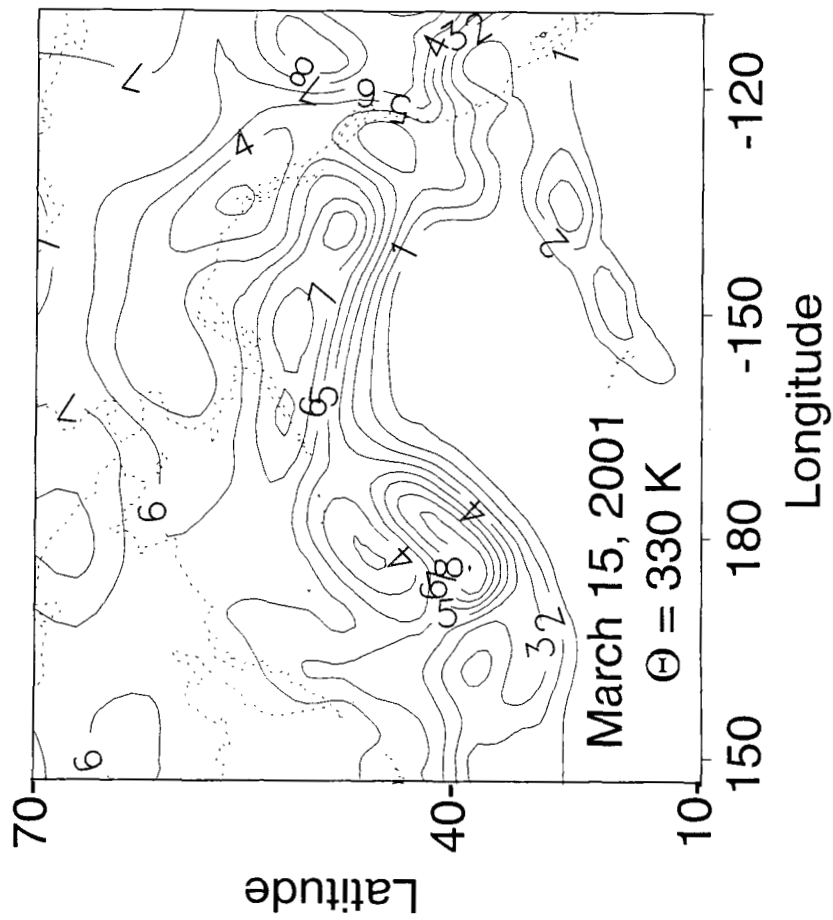


Figure 28: Potential vorticity on March 15, 2001 at 0600 GMT on the 330 K potential temperature surface.

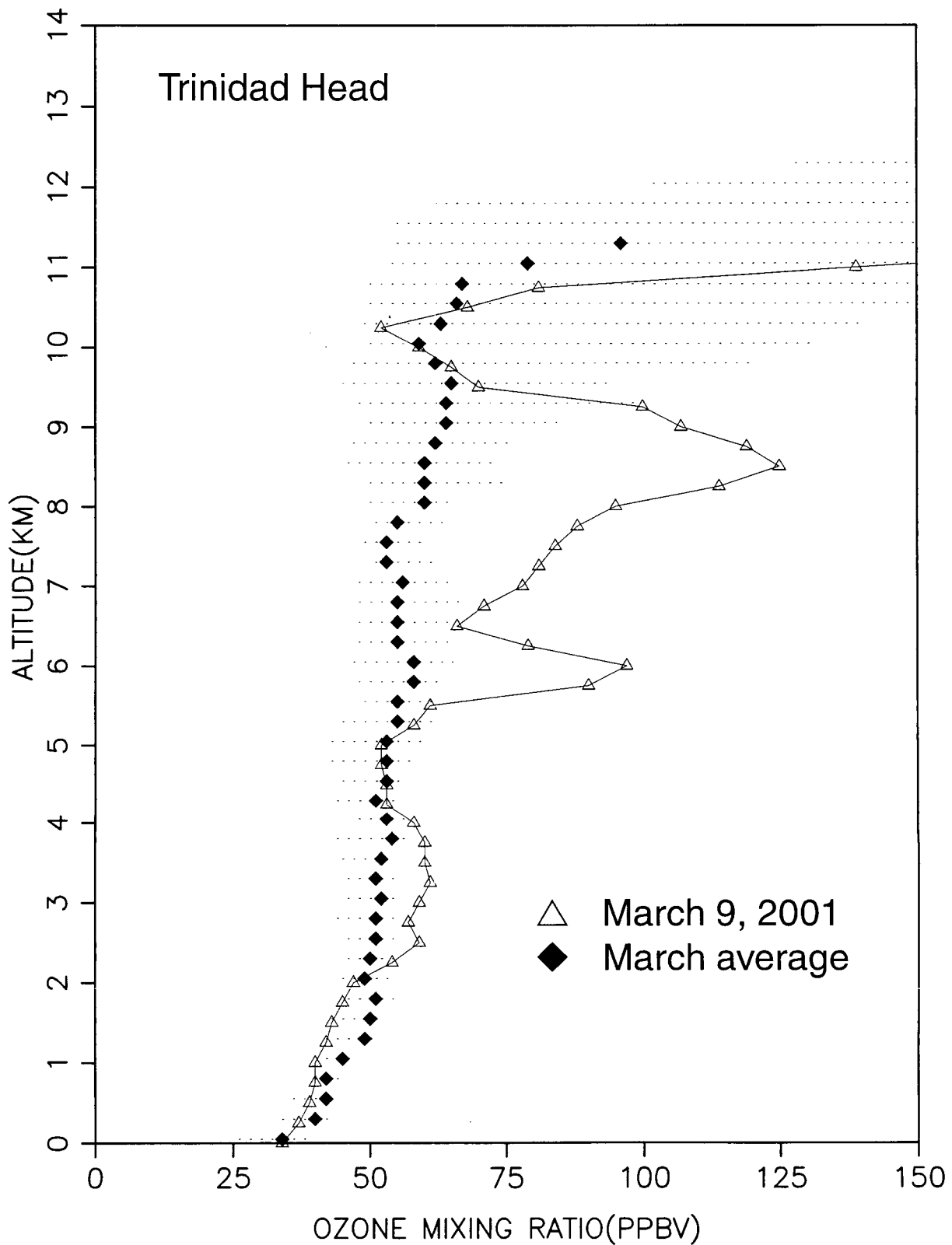


Figure 29: Profile of ozone mixing ratio at Trinidad Head on March 9, 2001. The multiyear average profile for March is also shown.

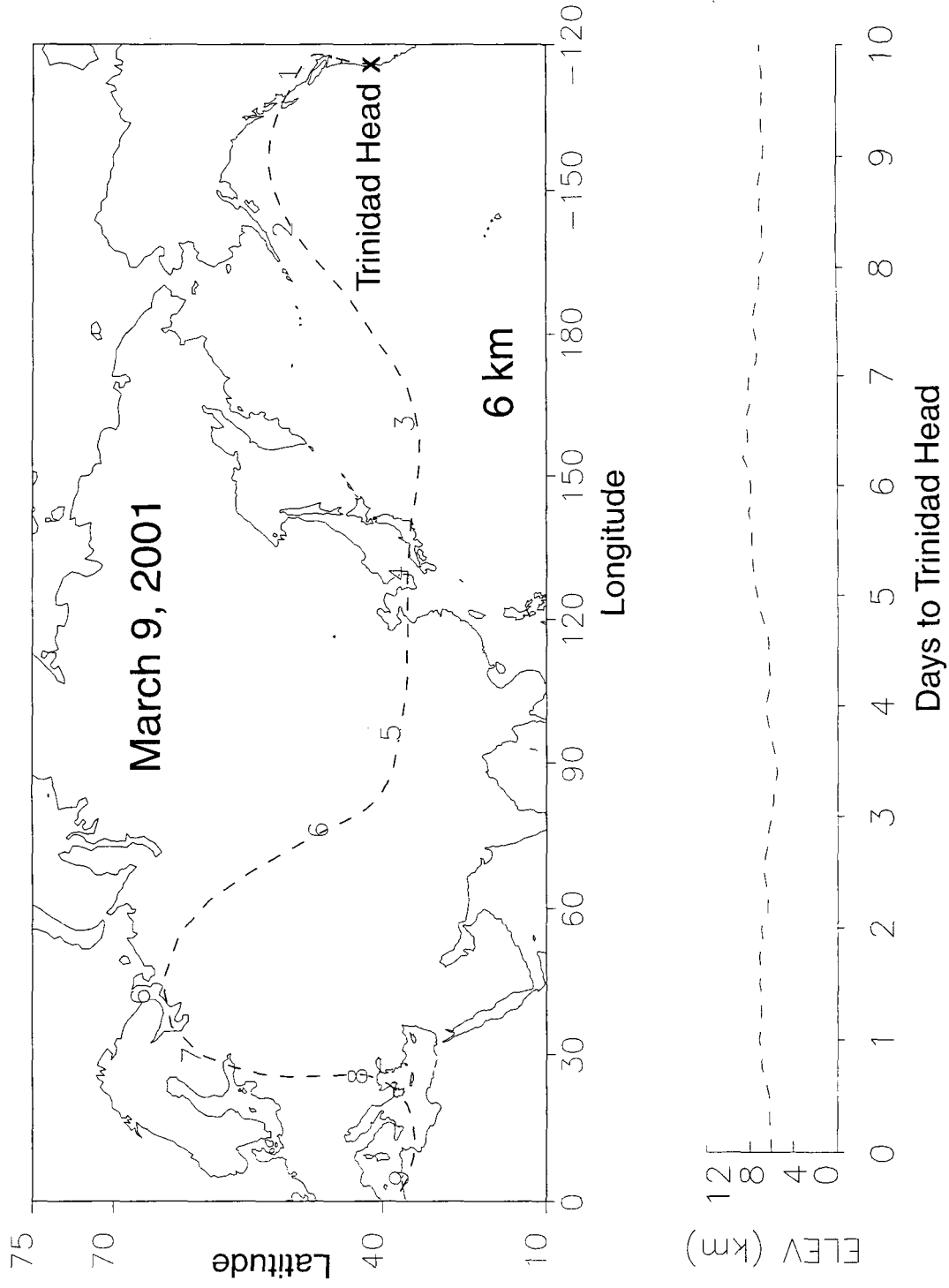


Figure 30: Isentropic, 10-day back trajectory to Trinidad Head on March 9, 2001 arriving at 6 km.

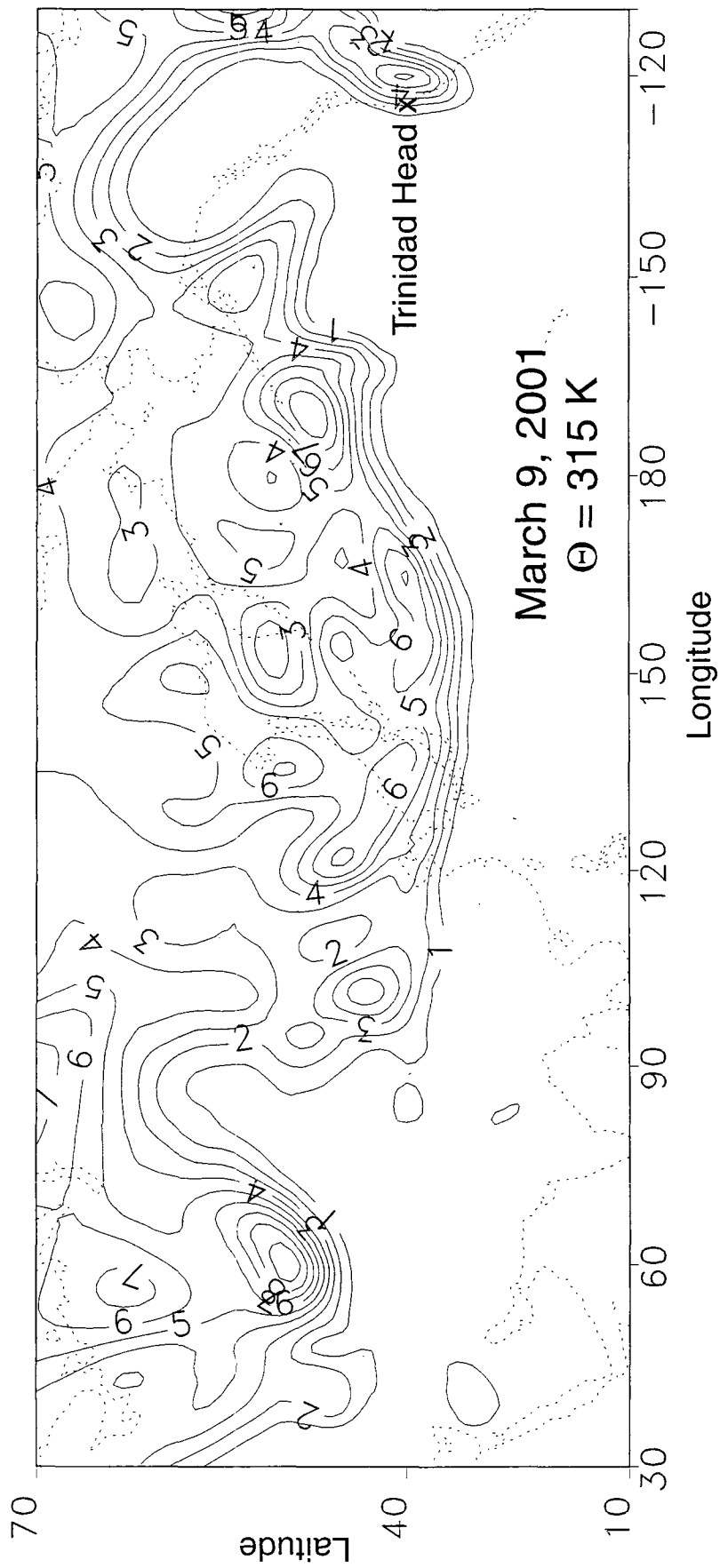


Figure 31: Potential vorticity on March 9, 2001 at 1800 GMT on the 300 K potential temperature surface.

**February 6, 2003**

**Popular Summary for Paper submitted to JGR-Atmospheres, TRACE-P Issue:**

**S. J. Oltmans, B. J. Johnson, J. M. Harris, A. M. Thompson, H. Y. Liu, H. Vömel, C. Y. Chan, T. Fujimoto, V. G. Brackett, W. L. Chang, J.-P. Chen, J. H. Kim, L. Y. Chan, H.-W. Chang, Tropospheric Ozone over the North Pacific from Ozonesonde Observations, *J. Geophys. Res.*, submitted, 2003.**

**S. Oltmans, B. Johnson, J. Harris, H. Voemel - NOAA/CMDL, Boulder CO**

**A M Thompson, NASA/GSFC, Code 916**

**V G Brackett, NASA/Langley**

**J-H Kim National Pusan University, Korea**

**Liu, Chan, Chang, Chen, Chan, Chang - Hong Kong University**

**During the (TRACE-P Transport and Chemical Evolution Experiment - Pacific) NASA experiment in the Pacific Rim and en route (Hawaii, Guam, Midway) there were many ozonesondes launched at Hong Kong, Hilo, Hawaii (with NASA and NOAA support). In addition, the routine soundings at 4 Japanese stations from 24N to 42 N were taking place. In this paper, a climatology of seasonal variations in ozone from data over the past 10 years is presented. Different patterns of pollution, stratospheric injection, clean air transport from tropical areas and convection are evident in the various sites. Soundings from coastal California (Trinidad Head) are not appreciably more polluted than those from northern Japan. Thus, one could conclude that on average intercontinental transport of ozone from Asia to North America is not dominant.**